Coordination compounds of cobalt(II) with carboxylate non–steroidal anti–inflammatory drugs: Structure and biological profile

Spyros Perontsis, Antonios G. Hatzidimitriou, and George Psomas *

Department of General and Inorganic Chemistry, Faculty of Chemistry, Aristotle University of Thessaloniki, GR–54124 Thessaloniki, Greece

* Corresponding author's e–mail: gepsomas@chem.auth.gr (G. Psomas)

Contents

S1 Antioxidant activity assay

The antioxidant activity of the compounds was evaluated *via* their ability to scavenge *in vitro* free radicals such as DPPH and ABTS and to reduce H_2O_2. All the experiments were carried out at least in triplicate and the standard deviation of absorbance was less than 10% of the mean.

S1.1 Determination of the reducing activity of the radical DPPH

To an ethanolic solution of DPPH (0.1 mM) an equal volume solution of the compounds (0.1 mM) in ethanol was added. Absolute ethanol was also used as control solution. The absorbance at 517 nm was recorded at room temperature after 30 and 60 min in order to examine the possible existence of a potential time-dependence of the DPPH radical scavenging activity [1]. The DPPH-scavenging activity of the compounds was expressed as the percentage reduction of the absorbance values of the initial DPPH solution (DPPH%). NDGA and BHT were used as reference compounds.

S1.2 Assay of radical cation ABTS-scavenging activity

The ABTS assay was performed to determine the activity of the compounds to scavenge the radical cation ABTS. Initially, a water solution of ABTS was prepared (2 mM). ABTS radical cation ($ABTS^{+\cdot}$) was produced by the reaction of ABTS stock solution with potassium persulfate (0.17 mM) and the mixture was stored in the dark at room temperature for 12-16 h before its use. The ABTS was oxidized incompletely because the stoichiometric reaction ratio of ABTS and potassium persulfate is 1:0.5. The absorbance became maximal and stable only after more than 6 h of reaction although the oxidation of the ABTS started immediately. The radical was stable in this form for more than 2 days when allowed to stand in the dark at room temperature. Afterwards, the $ABTS^{+\cdot}$ solution was diluted in ethanol to an absorbance of 0.70 at 734 nm and 10 μL of diluted compounds or standards (0.1 mM) in DMSO were added. The absorbance was recorded out exactly 1 min after initial mixing [1]. The ABTS radical scavenging activity was expressed as the percentage inhibition of the absorbance of the initial ABTS solution (ABTS%). Trolox was used as an appropriate standard.

S1.3 Reduction of hydrogen peroxide

The ability of the compounds to reduce hydrogen peroxide (H_2O_2) was estimated according to the method described in the literature [2]. The reaction mixture contained 20 μL of each of the tested compounds (0.1 mM) and 5 μL H_2O_2 solution (40 mM) in phosphate buffer (50 mM, pH 7.4). The absorbance was measured at 230 nm after 10 min. The antioxidant activity (reduction of hydrogen peroxide) of the compounds was expressed as the percentage decrease of the initial H_2O_2 solution (H_2O_2%). L-ascorbic acid (or vitamin C) was used as a standard.

S2 Binding studies with CT DNA

In order to study the interaction of complexes with DNA, the compounds were initially dissolved in DMSO (1 mM). Mixing of such solutions with the aqueous buffer solutions DNA or BSA used in the studies never exceeded 5% DMSO (v/v) in the final solution, which was needed due to low aqueous solubility of most compounds. In all experiments, the effect of DMSO on the data has been taken into consideration and the appropriate corrections have been performed. The interaction of the compounds with CT DNA was monitored by UV-vis spectroscopy, cyclic voltammetry, and viscosity measurements, and *via* competitive studies with EB by fluorescence emission spectroscopy.

S2.1 Binding study with CT DNA by UV-vis spectroscopy

The interaction of the compounds with CT DNA has been studied by UV-vis spectroscopy in order to investigate the possible binding modes to CT DNA and to calculate the DNA-binding constants (K_b). The K_b constants (in M^{-1}) were determined by the Wolfe-Shimer equation (equation S1) [3] and the plots [DNA]/(ε_A-ε_f) *versus* [DNA] using the UV-vis spectra of the complexes (20-30 μM) recorded for a constant concentration with increasing concentrations of CT DNA for diverse [complex]/[DNA] mixing ratios (= *r*). Control experiments with DMSO were performed and no changes in the spectra of CT DNA were observed. According to the Wolfe-Shimer equation (equation S1):

$$\frac{[DNA]}{(\varepsilon_A - \varepsilon_f)} = \frac{[DNA]}{(\varepsilon_b - \varepsilon_f)} + \frac{1}{K_b(\varepsilon_b - \varepsilon_f)} \qquad \text{(equation S1)}$$

where [DNA] is the concentration of DNA in base pairs, $\varepsilon_A = A_{obsd}/[compound]$, ε_f = the extinction coefficient for the free compound and ε_b = the extinction coefficient for the compound in the fully bound form. K_b is given by the ratio of slope to the y intercept in plots [DNA]/(ε_A-ε_f) *versus* [DNA].

S2.2 CT DNA–binding studies by cyclic voltammetry

The interaction of complexes **1**–**14** with CT DNA was also investigated *via* monitoring the changes observed in the cyclic voltammogram of a 0.33 mM 1:2 DMSO:buffer solution of the complex upon addition of DNA solution at diverse *r* values. The buffer was also used as the supporting electrolyte and the cyclic voltammograms were recorded at v = 100 mV s^{-1}. Cyclic voltammetry can be also used for the calculation of the corresponding equilibrium constant for the redox process. The ratio of the DNA–binding constants for the reduced (K_r) and oxidized forms (K_{ox}) of the complexes (K_r/K_{ox}) was calculated according to the equation S2 [4]:

$$\Delta E^o = E^o_{(b)} - E^o_{(f)} = 0.059 \times \log \frac{K_r}{K_{ox}} \qquad \text{(equation S2)}$$

where $E^o_{(b)}$ and $E^o_{(f)}$ are the formal potentials of Co(II)/Co(I) couple in the fully bound and free complexes, respectively. K_{ox} and K_r are the binding constants for the binding of the oxidized and reduced species to DNA, respectively.

S2.3 CT DNA-binding studies by viscosity measurements

The interaction of compounds with DNA has been evaluated *via* the study of the CT DNA viscosity ([DNA] = 0.1 mM) in a buffer solution (150 mM NaCl and 15 mM trisodium citrate at pH 7.0) in the presence of increasing amounts of the compounds (up to the value of r = 0.36). The obtained data are presented as $(\eta/\eta_0)^{1/3}$ *versus* r, where η is the viscosity of DNA in the presence of the compound, and η_0 is the viscosity of DNA alone in buffer solution.

S2.4 EB-displacement studies

The competition of the complexes with EB was investigated by fluorescence emission spectroscopy to examine whether the compounds can displace EB from its DNA-EB conjugate. The CT DNA-EB complex was formed by pre-treating 20 μM EB and 26 μM CT DNA in buffer (150 mM NaCl and 15 mM trisodium citrate at pH 7.0). The possible displacement of EB by the compounds and subsequently their intercalating effect was studied by the stepwise addition of a certain amount of the solution of each compound into the solution of the CT DNA-EB adduct. The solutions were excited at 540 nm and the emission was monitored from 550-700 nm with λ_{max} = 592-595 nm and the effect of the addition of each compound to the CT-DNA EB solution was recorded. The compounds do not display any fluorescence emission bands at room temperature in solution or in the presence of CT DNA or EB under the same experimental conditions ($\lambda_{excitation}$ = 540 nm); therefore, the observed quenching of the EB-DNA solution may be attributed to the displacement of EB from its EB-DNA adduct.

The Stern-Volmer constants (K_{SV}, in M^{-1}) were calculated according by the linear Stern-Volmer equation (equation S3) [5] and the respective plots Io/I *versus* [compound].

$$\frac{Io}{I} = 1 + k_q \tau_0 [Q] = 1 + K_{SV}[Q] \qquad \text{(equation S3)}$$

where Io and I are the emission intensities of the EB-DNA solution in the absence and the presence of the compounds, respectively, τ_o = the average lifetime of the emitting system without the quencher and kq = the quenching constant. Taking τ_o = 23 ns as the fluorescence lifetime of the EB-DNA

adduct [6], the quenching constants (k_q, in $M^{-1}s^{-1}$) of the compounds were calculated according to equation S4 [5]:

$$K_{SV} = k_q\tau_o \qquad \text{(equation S4)}$$

S3 Plasmid DNA cleavage experiments

The reaction mixtures (20 μL) containing supercoiled circular pBR322 plasmid DNA stock solution (Form I, 50 μM/base pair, ~500 ng), compounds, and Tris buffer (25 μM, pH 6.8) in Pyrex vials were incubated for 30 min at 37 °C and centrifuged under aerobic conditions at room temperature.

After addition of the gel-loading buffer [6x Orange DNA Loading Dye 10 mM Tris-HCl (pH 7.6), 0.15% orange G, 0.03% xylene cyanol FF, 60% glycerol, and 60 mM EDTA, by Fermentas], the reaction mixtures were loaded on a 1% agarose gel with EB staining. The electrophoresis tank was attached to a power supply at a constant current (75 V for 30 min). The gel was visualized by the Mupid-ONE LED Illuminator and photographed by a Nikon Digital Camera D3400. Quantification of DNA-cleaving activities was performed by integration of the optical density as a function of the band area using the program "Image J" available at the site http://rsb.info.nih.gov/ij/download.html.

The ss% and ds% damages were calculated according to the equations S5 and S6:

$$ss\% = \frac{FormII}{(FormI+FormII+FormIII)} \times 100 \qquad \text{(equation S5)}$$

$$ds\% = \frac{FormIII}{(FormI+FormII+FormIII)} \times 100 \qquad \text{(equation S6)}$$

where, as Form II we consider Form II of each series minus Form II of the irradiated control DNA and as Form I, we consider Form I of each series. The amount of supercoiled DNA was multiplied by factor of 1.43 to account for reduced EB intercalation into supercoiled DNA [7] .

S4 Albumin assays

S4.1 Albumin-binding studies

In order to investigate if the compounds can bind to carrier protein like serum albumins, we carried out albumin binding study by tryptophan fluorescence quenching experiments using bovine serum albumin (BSA, 3 μM) and human serum albumin (HSA, 3 μM) in buffer (containing 15 mM trisodium citrate and 150 mM NaCl at pH 7.0). The quenching of the emission intensity of tryptophan residues of BSA at 345 nm or HSA at 340 nm was monitored using the compounds as quenchers with increasing concentration [5]. The fluorescence emission spectra of the compounds were also recorded with λ_{ex} = 295 nm; in case that an additional emission band appeared the SA-fluorescence emission

spectra were corrected by subtracting the spectra of the compounds. The influence of the inner-filter effect [8] on the measurements was evaluated by equation S7.

$$I_{corr} = I_{meas} \times 10^{\frac{\varepsilon(\lambda_{exc})cd}{2}} \times 10^{\frac{\varepsilon(\lambda_{em})cd}{2}} \qquad \text{(equation S7)}$$

where I_{corr} = corrected intensity, I_{meas} = the measured intensity, c = the concentration of the quencher, d = the cuvette (1 cm), $\varepsilon_{(\lambda exc)}$ and $\varepsilon_{(\lambda em)}$ = the ε of the quencher at the excitation and the emission wavelength, respectively, as calculated from the UV-vis spectra of the compound [8].

The Stern-Volmer and Scatchard graphs are used to study the interaction of the compounds with serum albumins. According to Stern-Volmer quenching equation (equation S3), where Io = initial tryptophan fluorescence intensity of SA, I = tryptophan fluorescence intensity of SA after the addition of the quencher, k_q = quenching constant, K_{SV} = Stern-Volmer constant, τ_o = average lifetime of SA without the quencher, and, taking as fluorescence lifetime (τ_o) of tryptophan in SA at around 10^{-8} s [5], K_{SV} (in M^{-1}) can be obtained by the slope of the diagram Io/I *versus* [compound] (Stern-Volmer plots), and subsequently the quenching constants (k_q, in $M^{-1}s^{-1}$) may be calculated from equation S4.

From the Scatchard equation (equation S8):

$$\frac{\Delta I / Io}{[Q]} = nK - K\frac{\Delta I}{Io} \qquad \text{(equation S8)}$$

where n is the number of binding sites per albumin and K is the SA-binding constant (K, in M^{-1}) is calculated from the slope in plots (ΔI/Io)/[complex] *versus* ΔI/Io and n is given by the ratio of y intercept to the slope [9].

S4.2 Competitive SA-fluorescence studies with warfarin and ibuprofen

The competitive studies with warfarin or ibuprofen (site-markers)[10] were performed by tryptophan fluorescence quenching experiments using a fixed concentration of the albumin and site probes (3 μM) in buffer (containing 15 mM trisodium citrate and 150 mM NaCl at pH 7.0). The fluorescence emission spectra were recorded in the presence of increasing amounts of the compounds as quenchers with an excitation wavelength of 295 nm. The Scatchard equation (equation S8) [9] and plots were applied on the corrected SA-fluorescence emission spectra to determine the SA-binding constant of the compounds in the presence of warfarin or ibuprofen.

S5 References

1 C. Kontogiorgis and D. Hadjipavlou-Litina, *J Enzyme Inhib Med Chem*, 2003, **18**, 63–69.

2 R. J. Ruch, S. Cheng and J. E. Klaunig, *Carcinogenesis*, 1989, **10**, 1003–1008.
3 A. Wolfe, G. H. Shimer and T. Meehan, *Biochemistry*, 1987, **26**, 6392–6396.
4 M. T. Carter, M. Rodriguez and A. J. Bard, *J Am Chem Soc*, 1989, **111**, 8901–8911.
5 J. R. Lakowicz, *Principles of fluorescence spectroscopy*, Springer, 2006.
6 D. P. Heller and C. L. Greenstock, *Biophys Chem*, 1994, **50**, 305–312.
7 A. Papastergiou, S. Perontsis, P. Gritzapis, A. E. Koumbis, M. Koffa, G. Psomas and K. C. Fylaktakidou, *Photochemical and Photobiological Sciences*, 2016, **15**, 351–360.
8 L. Stella, A. L. Capodilupo and M. Bietti, *Chemical Communications*, 2008, 4744–4746.
9 Y.-Q. Wang, H.-M. Zhang, G.-C. Zhang, W.-H. Tao and S.-H. Tang, *J Lumin*, 2007, **126**, 211–218.
10 M. Lazou, A. Tarushi, P. Gritzapis and G. Psomas, *J Inorg Biochem*, 2020, **206**, 111019.

Table S1. Experimental X–ray crystallography details for complexes **1** and **2**.

	Complex **1**	Complex **2**
CCDC no	2336775	2336776
Crystal data		
Chemical formula	$C_{34}H_{30}Cl_2CoN_6O_4$	$C_{36}H_{36}CoN_6O_4$
M_r	716.49	675.65
Crystal system, space group	Monoclinic, $P2_1/n$	Monoclinic, $P2_1/n$
Temperature (K)	295	295
a, b, c (Å)	17.990(5), 7.8905(19), 24.355(6)	19.151(3), 7.9798(12), 22.577(4)
β (°)	98.540 (9)	100.057 (6)
V (Å^3)	3418.8 (15)	3397.2 (10)
Z	4	4
Radiation type	Mo $K\alpha$	Mo $K\alpha$
μ (mm^{-1})	0.71	0.55
Crystal size (mm)	0.15 × 0.14 × 0.06	0.26 × 0.18 × 0.17
Data collection		
Diffractometer	Bruker Kappa Apex2	
Absorption correction	Numerical / Analytical Absorption (De Meulenaer & Tompa, 1965)	
T_{min}, T_{max}	0.91, 0.96	0.91, 0.91
No. of measured reflections	32375	30478
No. of independent reflections	6531	6467
No. of observed [$I > 2.0\sigma(I)$] reflections	4605	4399
R_{int}	0.020	0.051
$(\sin\theta/\lambda)_{max}$ (Å^{-1})	0.616	0.612
Refinement		
$R[F^2 > 2\sigma(F^2)]$, $wR(F^2)$, S	0.037, 0.062, 1.00	0.050, 0.072, 1.00
No. of reflections	4605	4399
No. of parameters	424	424
H-atom treatment	H-atom parameters constrained	
$\Delta\rho_{max}$, $\Delta\rho_{min}$ (e Å^{-3})	0.40, −0.67	0.35, −0.41

Table S2. Experimental X–ray crystallography details for complexes **5** and **6**.

	Complex **5**	Complex **6**
CCDC no	2336777	2336778
Crystal data		
Chemical formula sum	$C_{48}H_{44}Cl_4CoN_6O_6$	$C_{61}H_{60}Cl_8Co_2N_6O_{15}$
Chemical formula moiety	$C_{38}H_{34}Cl_4CoN_4O_6$, $2(C_5H_5N)$	$C_{33}H_{32}Cl_4CoN_4O_7$, $C_{28}H_{28}Cl_4CoN_2O_8$
M_r	1001.66	1518.67
Crystal system, space group	Triclinic, *P*-1	Monoclinic, *C*2/*c*
Temperature (K)	295	295
a, *b*, *c* (Å)	9.9854 (14), 10.3306 (17), 13.136 (2)	37.393 (2), 9.5275 (5), 9.8887 (5)
α, β, γ (°)	111.673 (9), 91.634 (9), 109.250 (8)	90, 91.9463 (18), 90
V (Å^3)	1171.3 (3)	3521.0 (3)
Z	1	2
Radiation type	Mo *K*α	Mo *K*α
μ (mm^{-1})	0.65	0.84
Crystal size (mm)	0.26 × 0.18 × 0.17	0.26 × 0.25 × 0.21
Data collection		
Diffractometer	Bruker Kappa Apex2	
Absorption correction	Numerical / Analytical Absorption (De Meulenaer & Tompa, 1965)	
T_{min}, T_{max}	0.89, 0.90	0.81, 0.84
No. of measured reflections	23179	20090
No. of independent reflections	4530	3362
No. of observed [$I > 2.0\sigma(I)$] reflections	3205	2590
R_{int}	0.030	0.028
$(\sin\theta/\lambda)_{max}$ (Å^{-1})	0.617	0.613
Refinement		
$R[F^2 > 2\sigma(F^2)]$, $wR(F^2)$, S	0.045, 0.078, 1.00	0.058, 0.133, 1.00
No. of reflections	3205	2590
No. of parameters	295	221
No. of restraints	6	22
H-atom treatment	H-atom parameters constrained	
$\Delta\rho_{max}$, $\Delta\rho_{min}$ (e Å^{-3})	0.74, −0.37	0.84, −0.55

Table S3. Experimental X–ray crystallography details for complexes **8** and **9**.

	Complex **8**	Complex **9**
CCDC no	2336779	2336780
Crystal data		
Chemical formula	$C_{42}H_{34}Cl_2CoN_4O_4$	$C_{44}H_{40}CoN_4O_4$
M_r	788.59	747.76
Crystal system, space group	Monoclinic, $P2_1/c$	Triclinic, P-1
Temperature (K)	295	295
a, b, c (Å)	11.3476(8), 21.4206(15), 14.9086(9)	9.4414 (8), 12.2235 (13), 17.5565 (18)
α, β, γ (°)	90, 93.1479 (19), 90	102.832 (6), 97.905 (5), 107.314 (5)
V (Å^3)	3618.4 (4)	1840.3 (3)
Z	4	2
Radiation type	Mo $K\alpha$	Mo $K\alpha$
μ (mm^{-1})	0.67	0.52
Crystal size (mm)	0.22 × 0.15 × 0.14	0.21 × 0.19 × 0.13
Data collection		
Diffractometer	Bruker Kappa Apex2	
Absorption correction	Numerical / Analytical Absorption (De Meulenaer & Tompa, 1965)	
T_{min}, T_{max}	0.90, 0.91	0.90, 0.94
No. of measured reflections	44442	29698
No. of independent reflections	6865	6757
No. of observed [$I > 2.0\sigma(I)$] reflections	4956	5110
R_{int}	0.049	0.030
$(\sin\theta/\lambda)_{max}$ (Å^{-1})	0.611	0.605
Refinement		
$R[F^2 > 2\sigma(F^2)]$, $wR(F^2)$, S	0.047, 0.059, 1.00	0.042, 0.055, 1.00
No. of reflections	4956	5110
No. of parameters	478	478
H-atom treatment	H-atom parameters constrained	
$\Delta\rho_{max}$, $\Delta\rho_{min}$ (e Å^{-3})	0.45, −0.49	0.38, −0.34

Table S4. Experimental X–ray crystallography details for complexes **10** and **14**.

	Complex **10**	Complex **14**
CCDC no	2336781	2336782
Crystal data		
Chemical formula	$C_{42}H_{38}CoN_2O_6$	$C_{55}H_{40}Co_2F_4N_4O_7$
M_r	725.71	1062.80
Crystal system, space group	Monoclinic, $P2_1/c$	monoclinic, $C2/c$
Temperature (K)	295	295
a, b, c (Å)	12.7879 (16), 28.495 (4), 10.0793 (15)	31.461(19), 7.752(5), 21.744(13)
α, β, γ (°)	94.441 (4)	98.004(15)
V (Å^3)	3661.8 (9)	5252(5)
Z	4	4
Radiation type	Mo $K\alpha$	Mo $K\alpha$
μ (mm^{-1})	0.52	0.70
Crystal size (mm)	0.22 × 0.14 × 0.14	0.23 × 0.22 × 0.18
Data collection		
Diffractometer	Bruker Kappa Apex2	
Absorption correction	Numerical / Analytical Absorption (De Meulenaer & Tompa, 1965)	
T_{min}, T_{max}	0.93, 0.93	0.86, 0.88
No. of measured reflections	34918	20180
No. of independent reflections	6937	4985
No. of observed [$I > 2.0\sigma(I)$] reflections	5178	3934
R_{int}	0.007	0.017
$(\sin\theta/\lambda)_{max}$ (Å^{-1})	0.612	0.617
Refinement		
$R[F^2 > 2\sigma(F^2)]$, $wR(F^2)$, S	0.057, 0.084, 1.00	0.0515, 0.0869, 1.000
No. of reflections	5178	3934
No. of parameters	458	332
No. of restraints	5	2
H-atom treatment	H atoms treated by a mixture of independent and constrained refinement	H-atom parameters constrained
$\Delta\rho_{max}$, $\Delta\rho_{min}$ (e Å^{-3})	0.44, −0.59	0.65, −0.46

Table S5. Selected bond distances and angles for complexes **1** and **2**.

	Complex **1**	Complex **2**
Bond	**Distance (Å)**	**Distance (Å**
Co1—O1	1.980(2)	2.042(2)
Co1—O3	2.0078(18)	2.025(2)
Co1—N1	2.048(2)	2.051(3)
Co1—N3	2.025(2)	2.035(2)
Co1…O2	2.985	2.420(3)
Co1…O4	2.559	2.435(3)
Bonds	**Angle (º)**	**Angle (º)**
O1—Co1—O3	103.45(8)	102.79(10)
O1—Co1—N1	105.58(9)	95.64(11)
O1—Co1—N3	126.94(8)	143.01(11)
O3—Co1—N1	98.86(9)	104.74(10)
O3—Co1—N3	113.63(9)	104.45(9)
N1—Co1—N3	104.67(9)	101.05(11)

Table S6. Hydrogen-bond geometry in complexes **1**, **2, 5**, **6**, **8, 9** and **14**.

D*—H···*A	***D*—H (Å)**	**H···*A* (Å)**	***D*···*A* (Å)**	***D*—H···*A* (º)**	**Symmetry code**
1					
N2—H21···O1^{i}	0.87	2.25	2.955 (5)	138	(i) *x*, *y*−1, *z*
N5—H343···O2	0.85	2.10	2.792 (5)	138	
N4—H344···O4^{ii}	0.86	1.89	2.731 (5)	166	(ii) −*x*+1/2, *y*−1/2, −*z*+3/2
2					
N2—H21···O1^{i}	0.86	2.13	2.937 (5)	158	(i) *x*, *y*+1, *z*
N5—H51···O2	0.85	2.09	2.752 (5)	134	
N6—H363···O3	0.86	1.98	2.655 (5)	135	
N4—H364···O4^{ii}	0.86	1.95	2.788 (5)	166	(ii) −*x*+1/2, *y*+1/2, −*z*+1/2
5					
O3—H32···O2^{i}	0.82	1.84	2.636 (6)	163	(i) −*x*+1, −*y*+1, −*z*+1
N3—H242···O1	0.87	1.97	2.631 (6)	132	
O3—H243···N4	0.80	2.13	2.855 (6)	150	
6a					
N1—H11···O2	0.86	2.22	2.865 (9)	131	
N3—H32···O2^{ii}	0.85	2.38	3.176 (9)	155	(ii) *x*, *y*−1, *z*
O5—H53···O1^{v}	0.86	2.19	2.773 (9)	125	(v) −*x*+1, −*y*, −*z*
O5—H53···O3^{vi}	0.86	2.27	3.047 (9)	151	(vi) *x*, −*y*, *z*−1/2
O5—H53···N2^{v}	0.86	2.58	3.326 (9)	146	(v) −*x*+1, −*y*, −*z*
O6—H63···N3^{vii}	0.83	2.41	3.236 (9)	180	(vii) *x*, *y*+1, *z*
6b					
N1—H11···O2	0.86	2.22	2.865 (9)	131	
O3—H33···O1^{iv}	0.86	1.94	2.669 (9)	143	(iv) *x*, −*y*, *z*+1/2
O3—H35···O5^{iv}	0.86	2.35	3.047 (9)	139	(iv) *x*, −*y*, *z*+1/2
O4—H42···O2^{i}	0.86	1.72	2.519 (9)	153	(i) −*x*+1, *y*, −*z*+1/2
8					
N3—H1···O2	0.87	1.94	2.642 (4)	137	
N4—H42···O4	0.83	2.04	2.720 (4)	139	
9					
N3—H424···O2	0.86	2.10	2.686 (4)	125	
N4—H425···O3	0.84	1.94	2.620 (4)	137	
14					
O4—H51···O5	0.81	0.86	1.525 (7)	132	
O4—H51···O5^{ii}	0.81	1.96	2.766 (7)	176	(ii) −*x*+1/2, −*y*+1/2, −*z*

Table S7. Selected bond distances and angles for complex **5**.

Bond	**Distance (Å)**
Co1—O1	2.094(2)
Co1—O3	2.097(2)
Co1—N2	2.201(3)
Bonds	**Angle (°)**
O1—Co1—O3	89.49(9)
O1—Co1—N2	88.18(9)
O3—Co1—N2	90.42(9)

Symmetry code: (i) −*x*+1, −*y*+1, −*z*+1

Table S8. Selected bond distances and angles for complex **6** (**6a** and **6b**).

	6a		**6b**
Bond	**Distance (Å)**	**Bond**	**Distance (Å)**
Co1—O1	2.100(3)	Co1—O1	2.100(3)
Co1—N2	2.095(11)	Co1—O3	2.103(11)
Co1—O5	2.110(7)	Co1—O4	2.065(12)
Co1—O6	2.170(14)		
Bonds	**Angle (º)**	**Bonds**	**Angle (º)**
$O1^{i}$—Co1—O1	178.9(2)	$O1^{i}$—Co1—O1	178.9(2)
O1—Co1—O5	89.5(2)	O1—Co1—O3	88.4(3)
O1—Co1—$O5^{i}$	90.6(2)	O1—Co1—O4	88.5(3)
O1—Co1—O6	86.6(5)	O3—Co1—O4	174.2(5)
O1—Co1—N2	88.3(3)	$O3^{i}$—Co1—O3	87.1(6)
O5—Co1—$O5^{i}$	167.4(4)	$O4^{i}$—Co1—O4	97.0(7)
O5—Co1—O6	93.2(4)	$O1^{i}$—Co1—$O4^{i}$	88.5(3)
O5—Co1—N2	89.4(4)	$O1^{i}$—Co1—O3	90.8(3)
O6—Co1—N2	174.2(6)		

Symmetry code: (i) $-x+1, y, -z+1/2$.

Table S9. Selected bond distances and angles for complexes **8–10**.

Complex	**8**	**9**	**10**
Bond	**Distance (Å)**	**Distance (Å)**	**Distance (Å)**
Co1—O1	2.1032(19)	2.0630(15)	2.031 (2)
Co1—O2	2.2034(18)	2.2472(15)	2.260 (2)
Co1—O3 or O5 [a]	2.1105(19)	2.1067(16)	2.172 (2)
Co1—O4	2.2365(19)	2.1869(17)	2.151 (2)
Co1—N1	2.126(2)	2.0966(18)	2.121 (3)
Co1—N2	2.104(2)	2.1135(18)	2.110 (3)
Bonds	**Angle (º)**	**Angle (º)**	**Angle (º)**
O1—Co1—O2	60.80(7)	59.98(6)	57.58(8)
O1—Co1—O3 or O5 [a]	92.22(8)	164.11(6)	103.86(9)
O1—Co1—O4	147.61(7)	108.14(6)	160.99(9)
O1—Co1—N1	94.62(8)	108.48(7)	105.81(10)
O1—Co1—N2	100.78(8)	91.61(6)	91.85(9)
O2—Co1—O3 or O5 [a]	83.76(8)	107.46(6)	85.41(8)
O2—Co1—O4	96.92(7)	91.04(6)	110.76(8)
O2—Co1—N1	154.72(8)	105.69(7)	101.29(10)
O2—Co1—N2	98.27(8)	151.50(6)	148.78(9)
O4—Co1—O3 or O5 [a]	60.28(7)	60.13(6)	58.28(8)
O4—Co1—N1	107.95(8)	143.34(6)	90.78(9)
O4—Co1—N2	105.84(8)	100.91(7)	100.41(9)
N1—Co1—O3 or O5 [a]	104.41(8)	83.57(7)	148.33(9)
N1—Co1—N2	79.57(8)	79.79(7)	79.59(11)
N2—Co1— O3 or O5 [a]	166.11(8)	100.91(7)	110.39(10)

[a] O3 for **8** and **9**; O5 for **10**.

Table S10. Selected bond distances and angles for complex **14**.

Bond	**Distance (Å)**	**Bond**	**Distance (Å)**
Co1—O1	1.967(2)	Co1—N1	2.083(3)
Co1—O3	2.051(2)	Co1—N2	2.073(3)
Co1—O3^{i}	1.997(2)	Co1…Co1^{i}	3.114
Bonds	**Angle (º)**	**Bonds**	**Angle (º)**
N1—Co1—N2	80.83(11)	N2—Co1—O1	104.30(11)
N1—Co1—O1	87.59(11)	N2—Co1—O3	119.94(10)
N1—Co1—O3	159.05(9)	N2—Co1—O3^{i}	110.74(10)
N1—Co1—O3^{i}	91.96(10)	O1—Co1—O3	89.40(10)
O3—Co1—O3^{i}	78.62(11)	O1—Co1—O3^{i}	144.43(9)

Symmetry code: (i) −*x*+1, *y*, −*z*+1/2.

Table S11. % DPPH–scavenging ability (DPPH%), % ABTS radical scavenging activity (ABTS%) and H_2O_2 reducing activity (H_2O_2%) for the compounds. All measurements were carried out in triplicate.

Compound	DPPH % (30 min)	DPPH% (60 min)	ABTS%	H_2O_2 %
Complex **1**	30.18±0.28	36.44±0.11	98.48±0.13	86.28±0.13
Complex **2**	10.15±0.35	8.75±0.25	98.71±0.14	88.57±0.16
Complex **3**	10.30±0.10	8.30±0.30	38.64±0.50	94.28±0.85
Complex **4**	14.42±0.27	18.92±0.08	72.79±0.50	87.17±0.54
Complex **5**	19.13±0.38	18.50±0.33	61.55±0.19	85.27±0.23
Complex **6**	19.91±0.55	18.68±0.59	99.07±0.07	88.57±0.16
Complex **7**	15.92±0.19	20.77±0.12	72.00±0.57	83.73±0.11
Complex **8**	26.31±0.46	25.50±0.35	95.71±0.43	89.54±0.52
Complex **9**	12.92±0.38	13.15±0.15	97.81±0.06	89.22±0.46
Complex **10**	10.20±0.50	8.10±0.10	38.29±0.29	98.64±0.90
Complex **11**	18.59±0.14	19.41±0.09	84.33±0.32	88.77±0.11
Complex **12**	22.19±0.35	23.77±0.54	85.00±0.38	88.39±0.14
Complex **13**	15.73±0.27	17.19±0.19	82.64±0.21	88.14±0.12
Complex **14**	15.95±0.14	14.36±0.27	67.79±0.36	92.07±0.53
Htolf [1]	14.57±0.62	17.86±0.54	59.43±0.33	75.26±0.29
Hmef [2]	5.72±0.08	11.74±0.20	92.51±0.44	76.42±0.21
Hnap [3]	8.03±0.32	8.43± 0.20	87.51±0.17	91.41±0.41
Na meclf [4]	27.78±0.56	29.15±0.76	27.07±0.06	72.88±0.40
Na dicl [5]	18.26±0.60	17.43±0.23	76.35±0.75	76.78±0.17
H_2difl [6]	10.42±0.56	14.31±0.45	76.58±0.74	78.46±0.08
NDGA	86.99±0.06	87.35±0.05	Not tested	Not tested
BHT	31.30±0.10	60.00±0.38	Not tested	Not tested
Trolox	Not tested	Not tested	98.10±0.48	Not tested
L–ascorbic acid	Not tested	Not tested	Not tested	60.80±0.20

References

1 S. Tsiliou, L. A. Kefala, F. Perdih, I. Turel, D. P. Kessissoglou and G. Psomas, *Eur J Med Chem*, 2012, **48**, 132–142.

2 F. Dimiza, A. N. Papadopoulos, V. Tangoulis, V. Psycharis, C. P. Raptopoulou, D. P. Kessissoglou and G. Psomas, *Dalton Transactions*, 2010, **39**, 4517–4528.

3 F. Dimiza, A. N. Papadopoulos, V. Tangoulis, V. Psycharis, C. P. Raptopoulou, D. P. Kessissoglou and G. Psomas, *J Inorg Biochem*, 2012, **107**, 54–64.

4 A. Barmpa, A. G. Hatzidimitriou and G. Psomas, *J Inorg Biochem*, 2021, **217**, 111357.

5 S. Perontsis, A. Dimitriou, P. Fotiadou, A. G. Hatzidimitriou, A. N. Papadopoulos and G. Psomas, *J Inorg Biochem*, 2019, **196**, 110688.

6 S. Tsiliou, L. A. Kefala, A. G. Hatzidimitriou, D. P. Kessissoglou, F. Perdih, A. N. Papadopoulos, I. Turel and G. Psomas, *J Inorg Biochem*, 2016, **160**, 125–139.

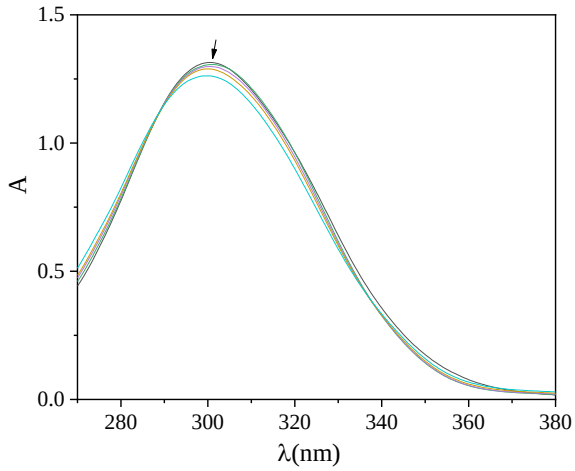

Complex **1**

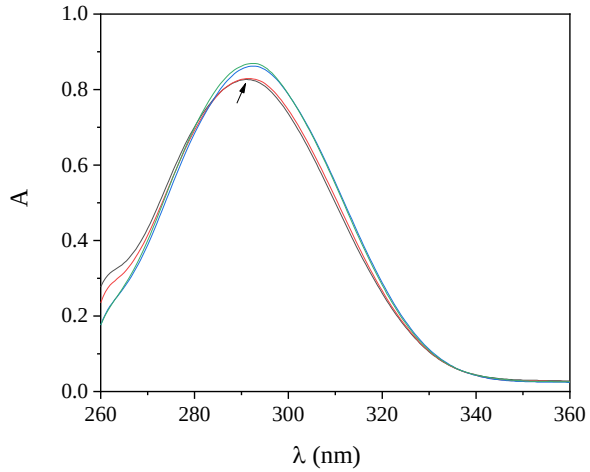

Complex **6**

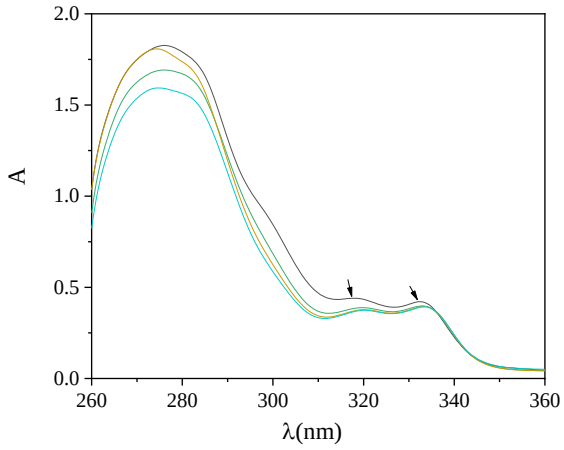

Complex **10**

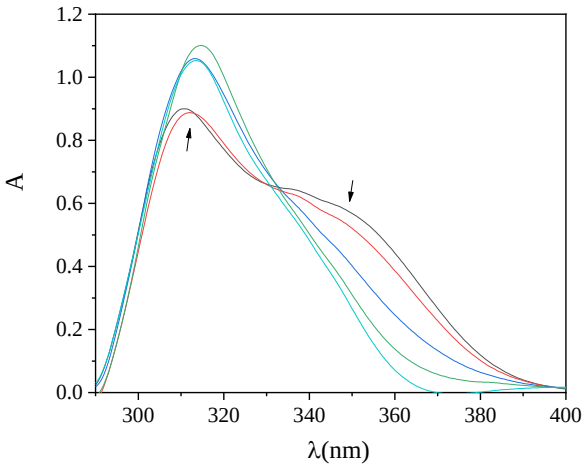

Complex **11**

Figure S1. UV–vis spectra of a DMSO solution of complexes **1, 6, 10**, and **11** in the presence of increasing amounts of CT DNA. The arrows show the changes upon increasing amounts of CT DNA.

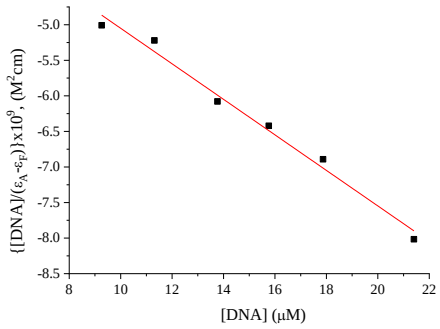

Complex **1**

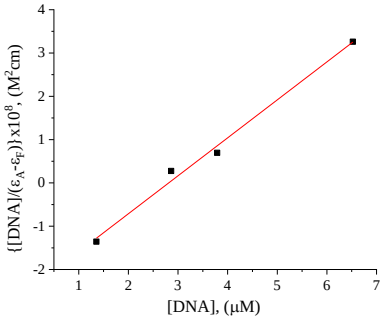

Complex **2**

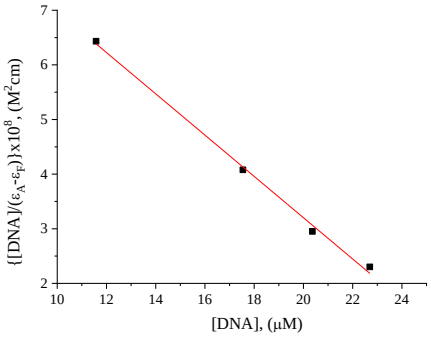

Complex **3**

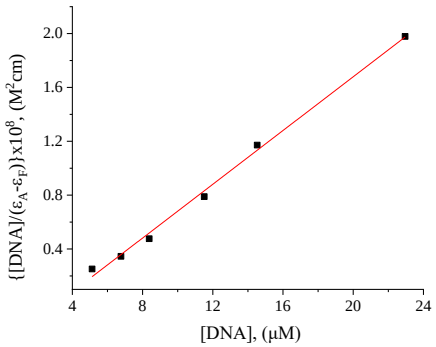

Complex **4**

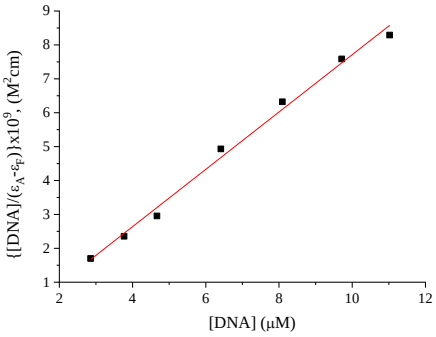

Complex **5**

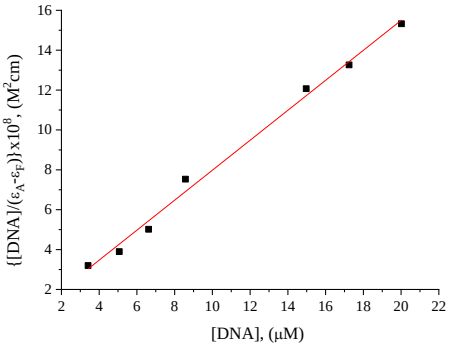

Complex **6**

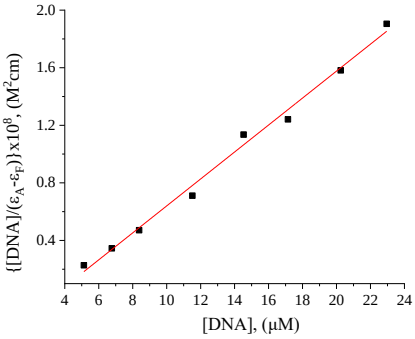

Complex **7**

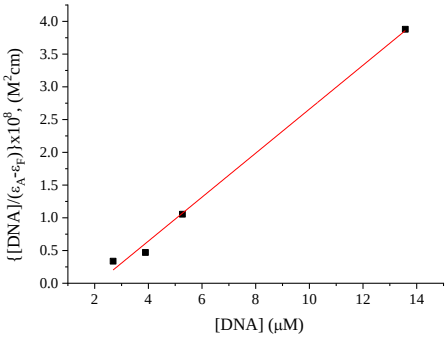

Complex **8**

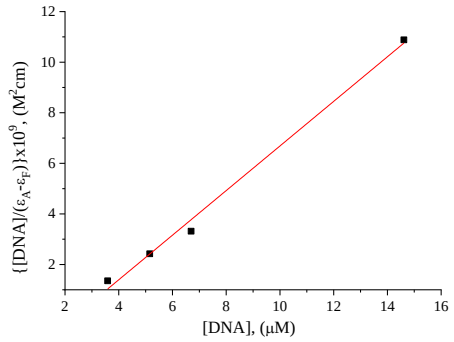

Complex **9**

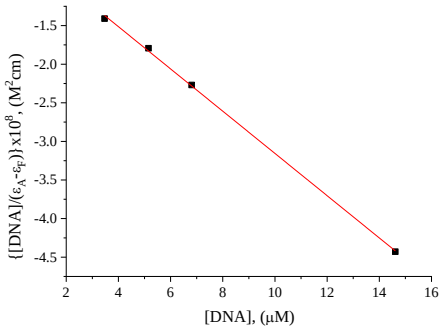

Complex **10**

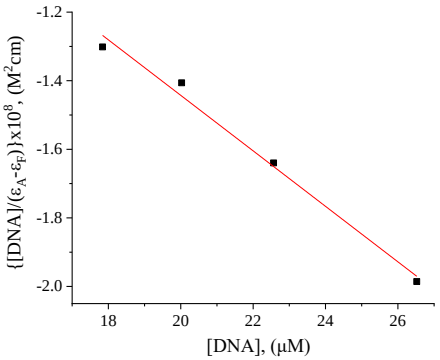

Complex **11**

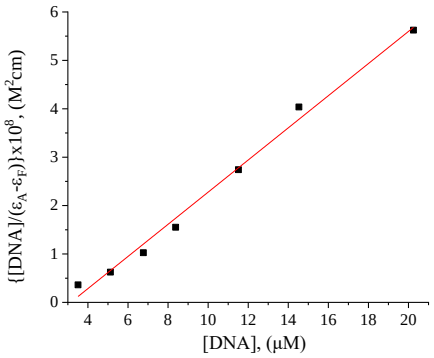

Complex **12**

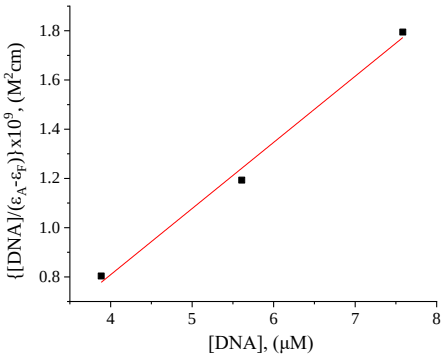

Complex **13**

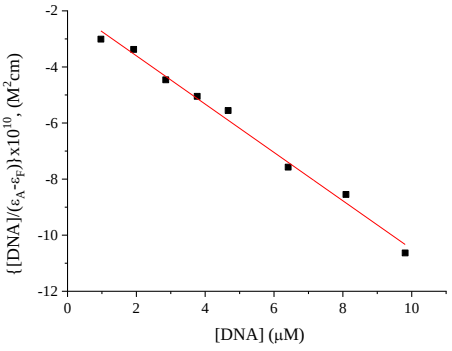

Complex **14**

Figure S2. Plots of [DNA]/(ε_A–ε_f) *versus* [DNA] for complexes **1-14**.

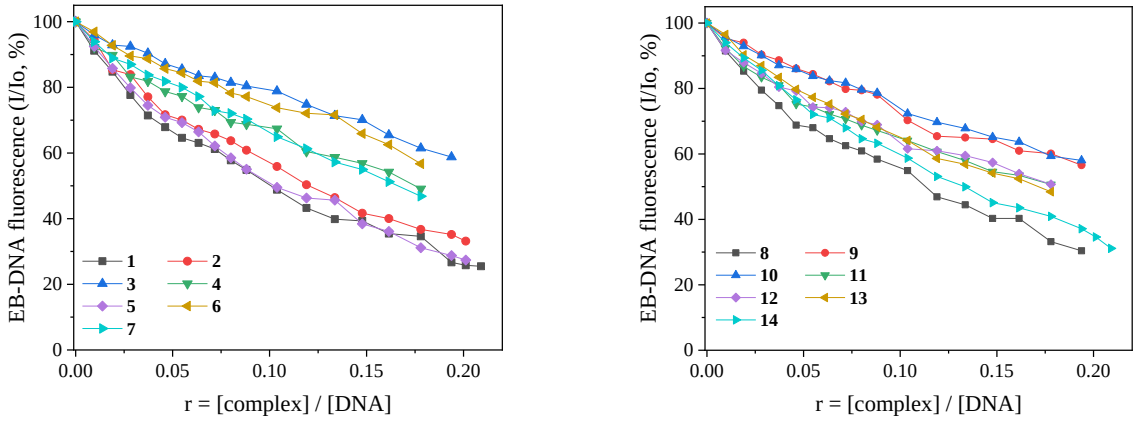

Figure S3. Plot of EB–DNA relative fluorescence emission intensity at $\lambda_{emission}$ = 592 nm (I/Io, %) *versus* r (r = [complex]/[DNA]) in the presence of complexes **1–14** (up to 25.5 % of the initial EB–DNA fluorescence emission intensity for **1**, 33.2 % for **2**, 58.8 % for **3**, 49.1% for **4,** 27.4 % for **5**, 56.7 % for **6**, 46.8% for **7,** 30.4 % for **8**, 56.6 % for **9**, 58.0% for **10,** 50.6 % for **11**, 50.7 % for **12**, 48.4% for **13,** and 31.1% for **14**).

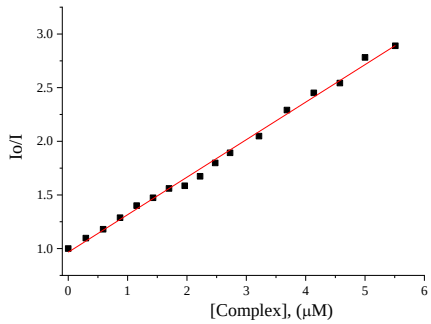

Complex **1**

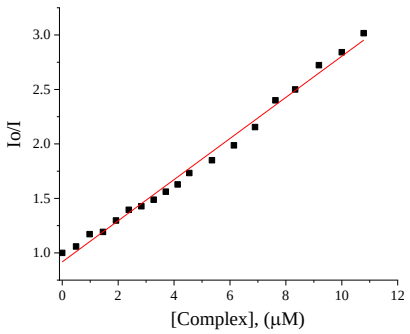

Complex **2**

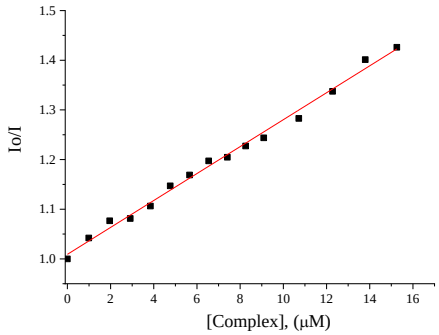

Complex **3**

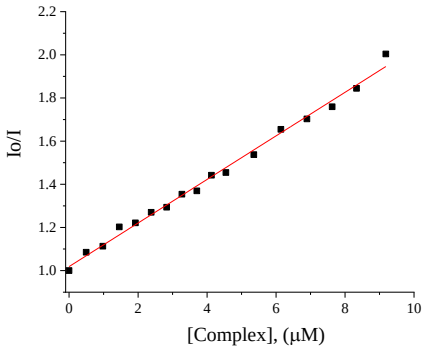

Complex **4**

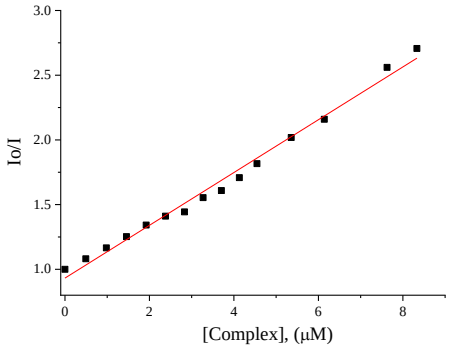

Complex **5**

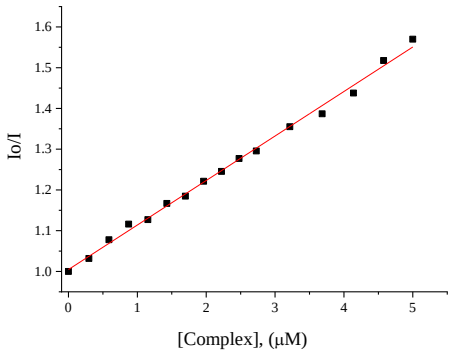

Complex **6**

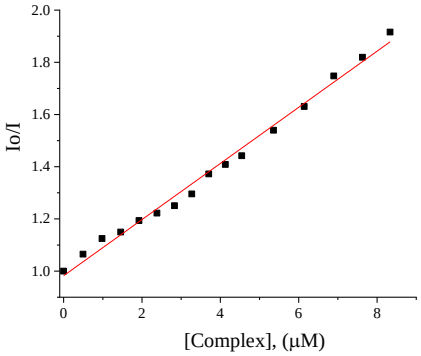

Complex **7**

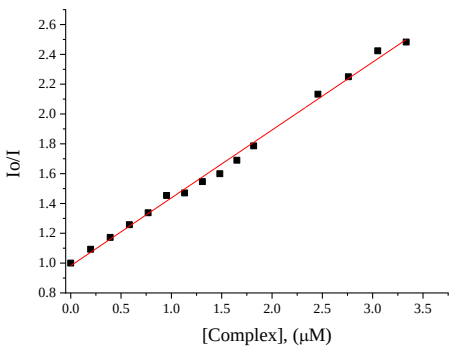

Complex **8**

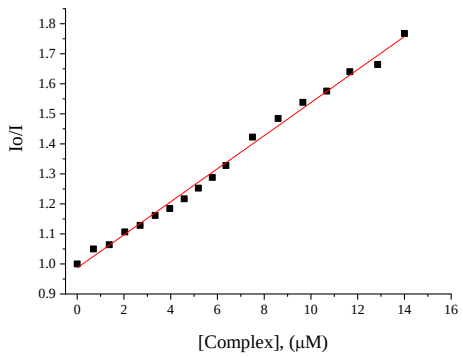

Complex **9**

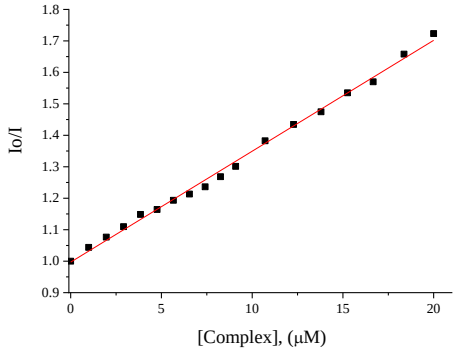

Complex **10**

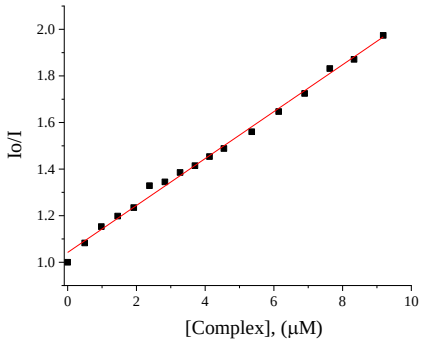

Complex **11**

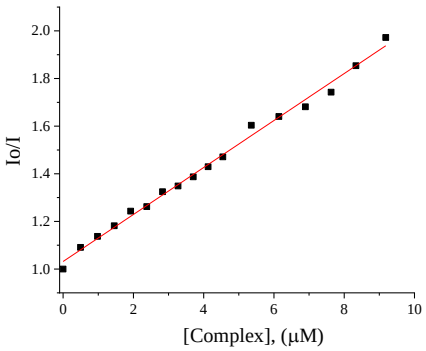

Complex **12**

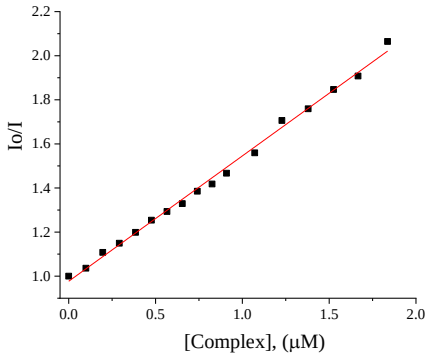

Complex **13**

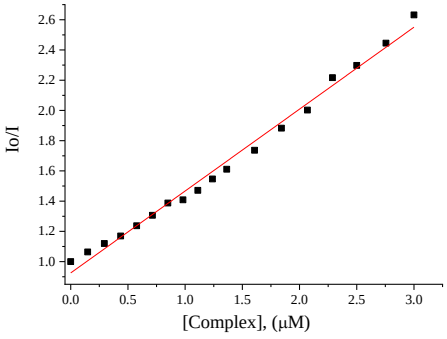

Complex **14**

Figure S4. Stern-Volmer plots of the EB-DNA quenching experiments upon addition of complexes **1-14**.

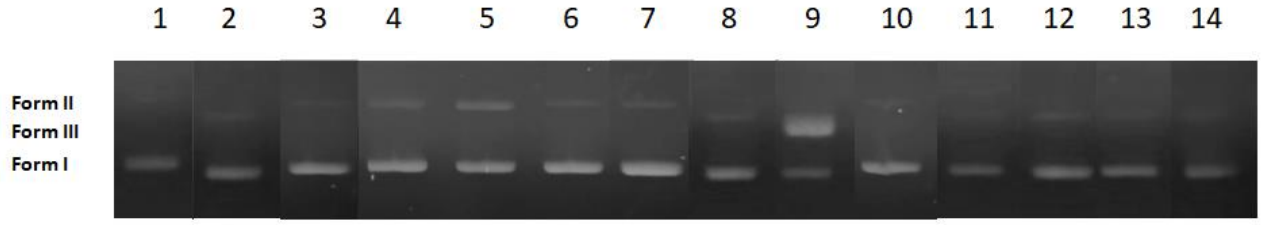

Form II	14	0	6	5	2	0	0	35	0	0	9	2	2
Form III	0	0	0	0	0	0	0	0	0	0	0	0	0

Figure S5. Agarose gel electrophoretic pattern of plasmid DNA (pBR322 DNA) with complexes **1–13** at 500 μM. Top: Gel electrophoreses pictures. Lane 1: DNA; Lane 2: DNA + complex **6**; Lane 3: DNA + complex **7**; Lane 4: DNA + complex **11**; Lane 5: DNA + complex **12**; Lane 6: DNA + complex **13**; Lane 7: DNA + complex **5**; Lane 8: DNA + complex **4**; Lane 9: DNA + complex **8**; Lane 10: DNA + complex **1**; Lane 11: DNA + complex **9;** Lane 12: DNA + complex **2**; Lane 13: DNA + complex **10**; Lane 14: DNA + complex **3**. Bottom: Calculation of the % conversion to ss and ds damage. DNA forms: Form I = supercoiled, Form II = relaxed, Form III = linear plasmid DNA.

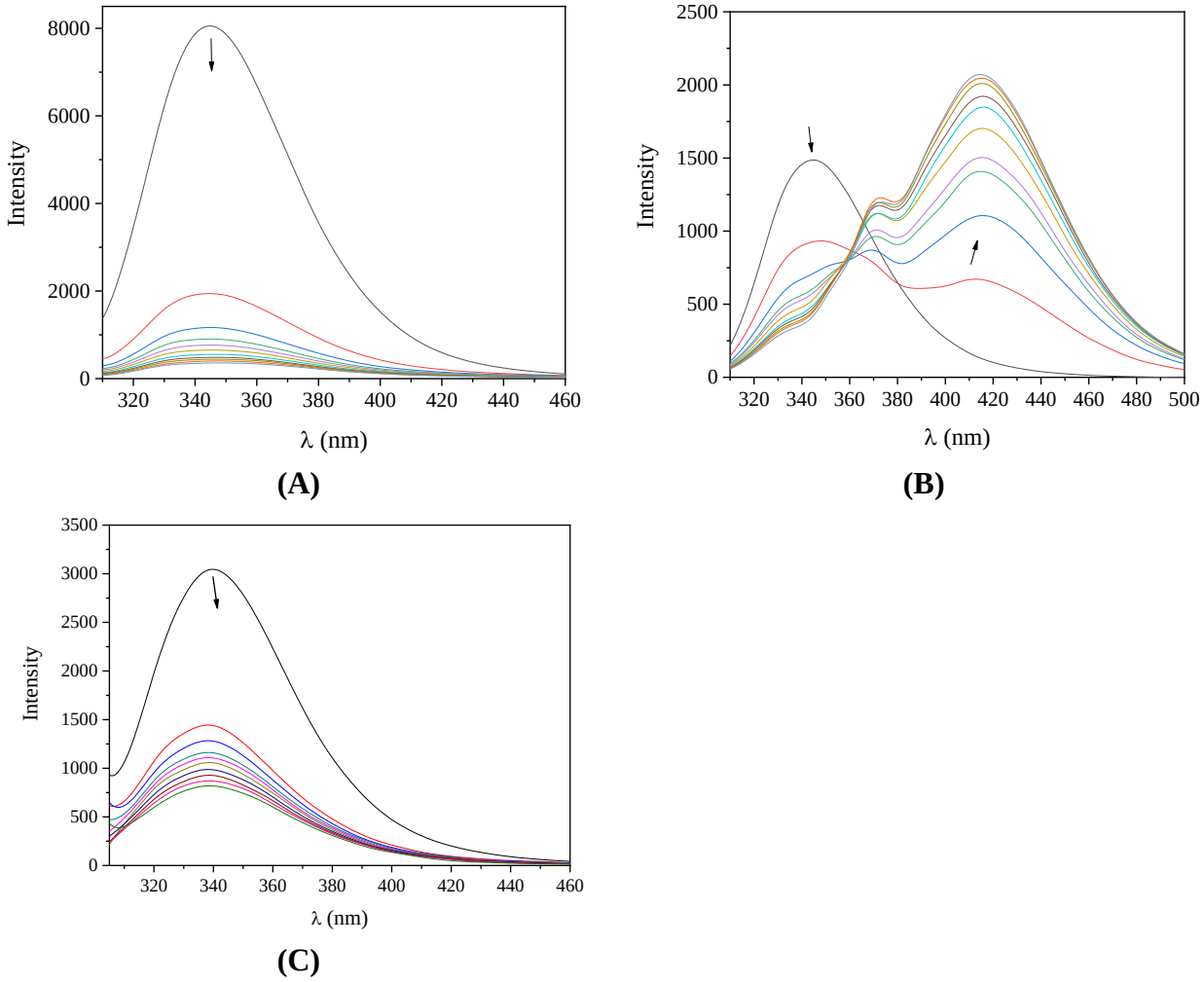

Figure S6. (A) and (B) Fluorescence emission spectra ($\lambda_{excitation}$ = 295 nm) for BSA (3 μM) in buffer solution (150 mM NaCl and 15 mM trisodium citrate at pH = 7.0) in the presence of increasing amounts (up to r = [complex]/[BSA] = 6.1) of (A) complex **1** or (B) complex **14**. (C) Fluorescence emission spectra ($\lambda_{excitation}$ = 295 nm) for HSA (3 μM) in buffer solution (150 mM NaCl and 15 mM trisodium citrate at pH = 7.0) in the absence and presence of increasing amounts (up to r = [complex]/[HSA] = 6.1) of complex **1**. The arrows show the changes of intensity upon increasing amounts of the complexes.

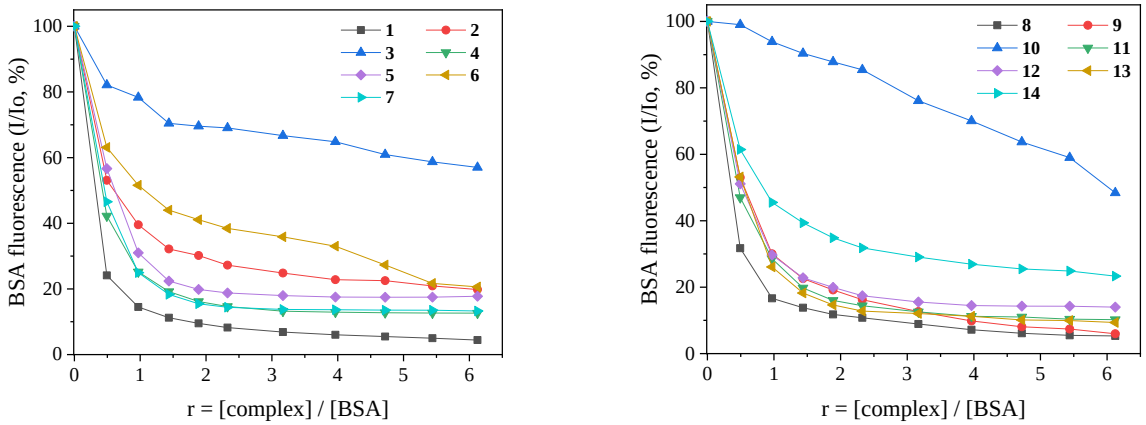

Figure S7. Plot of % relative fluorescence intensity at λ_{em} = 345 nm (I/Io, %) *versus r* (*r* = [complex]/[BSA]) for complexes **1-14** (up to 4.4% of the initial BSA fluorescence for **1**, 19.8 % for **2**, 57.0 % for **3**, 12.6% for **4,** 17.7 % for **5**, 20.6 % for **6**, 13.3% for **7,** 5.3 % for **8**, 6.0 % for **9**, 48.4% for **10,** 10.2 % for **11**, 14.0 % for **12**, 9.4% for **13,** and 23.3% for **14**).

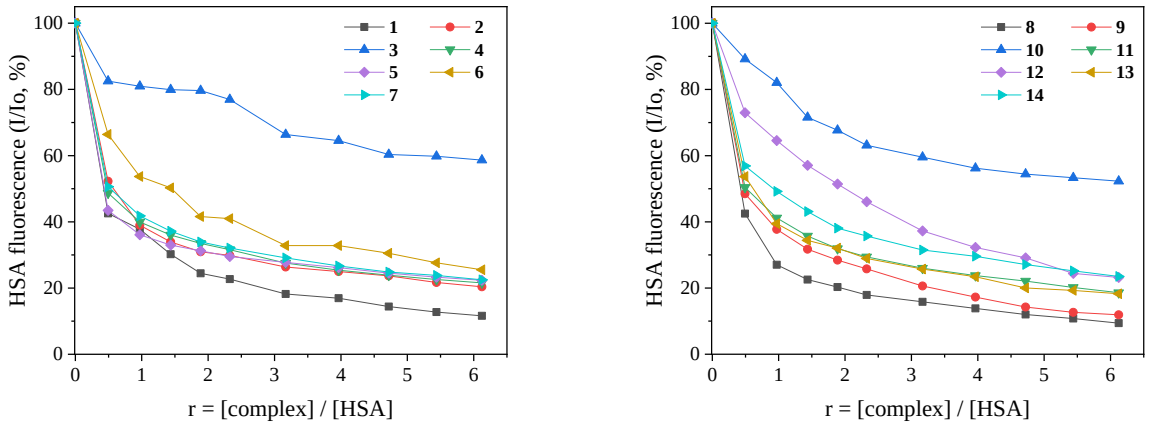

Figure S8. Plot of % relative fluorescence intensity at λ_{em} = 340 nm (I/Io, %) *versus* *r* (*r* = [complex]/[HSA]) for complexes **1-14** (up to 11.6% of the initial HSA fluorescence for **1**, 20.4 % for **2**, 58.6 % for **3**, 21.6% for **4,** 22.4 % for **5**, 25.5 % for **6**, 22.5% for **7,** 9.4 % for **8**, 11.9 % for **9**, 52.3% for **10,** 18.6 % for **11**, 23.2 % for **12**, 18.3% for **13,** and 23.5% for **14**).

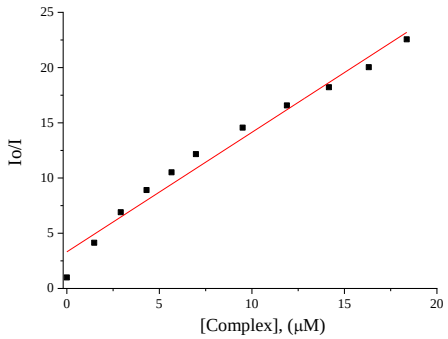

Complex **1**

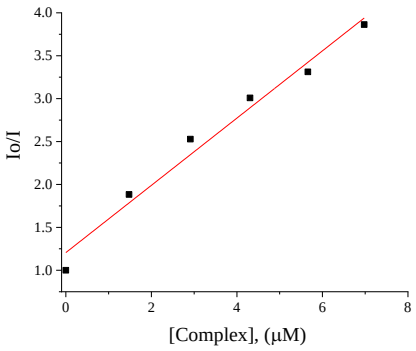

Complex **2**

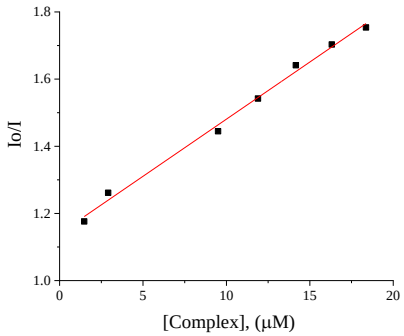

Complex **3**

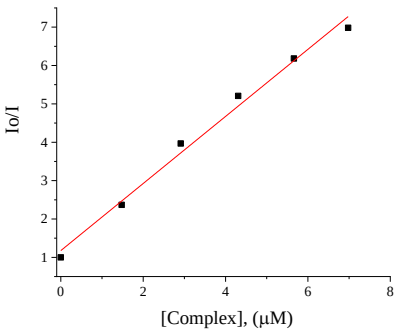

Complex **4**

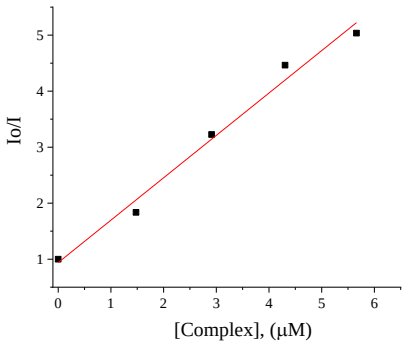

Complex **5**

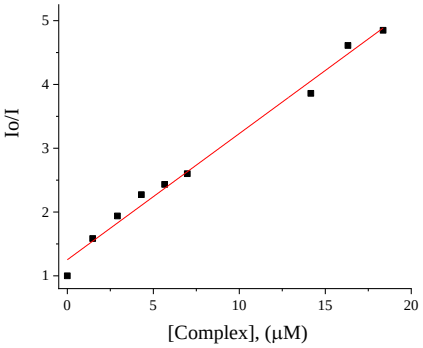

Complex **6**

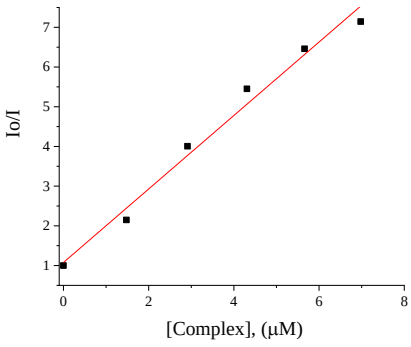

Complex **7**

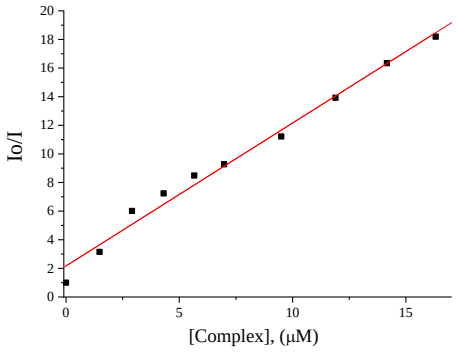

Complex **8**

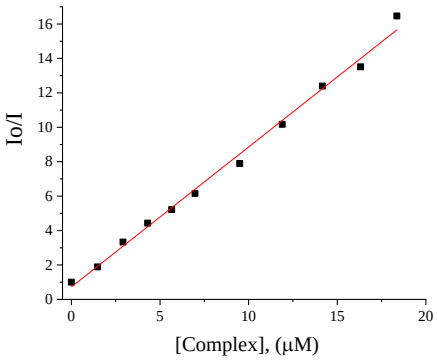

Complex **9**

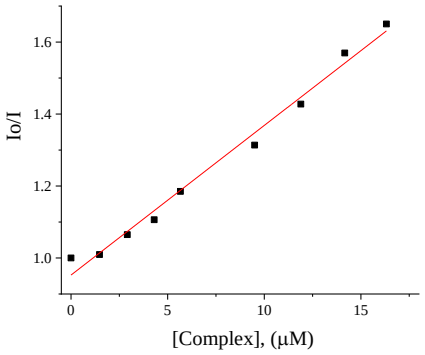

Complex **10**

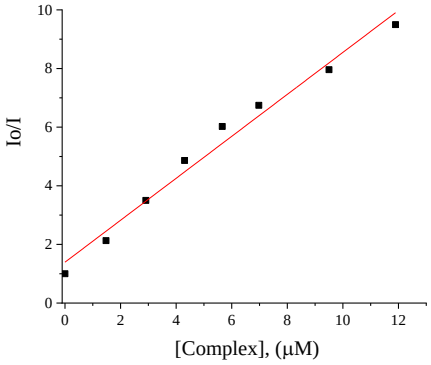

Complex **11**

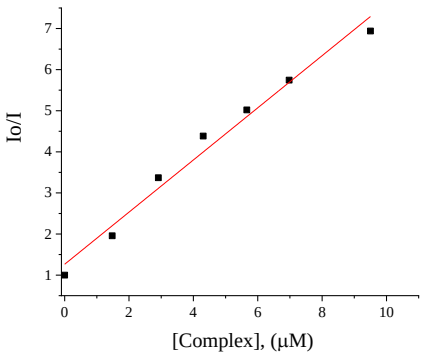

Complex **12**

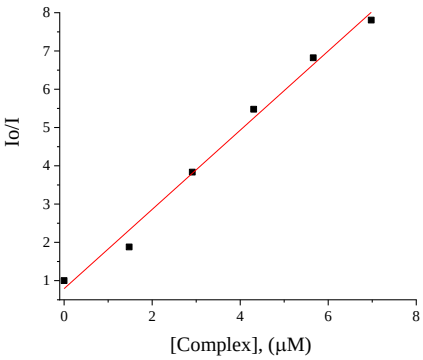

Complex **13**

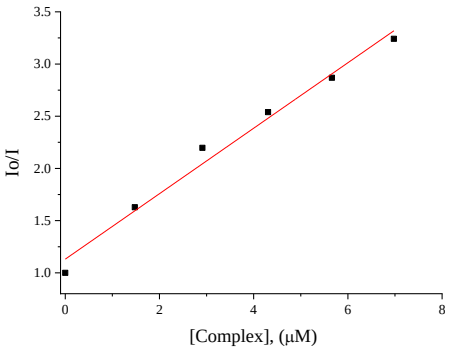

Complex **14**

Figure S9. Stern-Volmer plots of the BSA quenching experiments upon addition of complexes **1-14**.

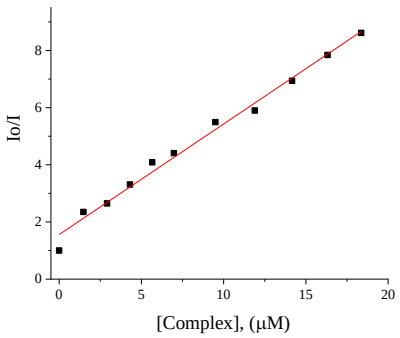

Complex **1**

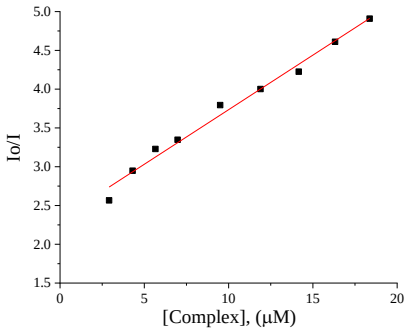

Complex **2**

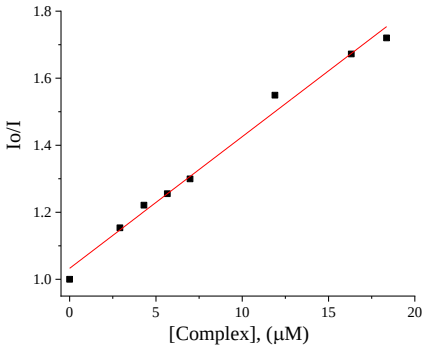

Complex **3**

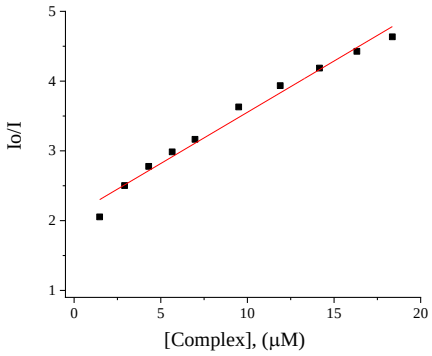

Complex **4**

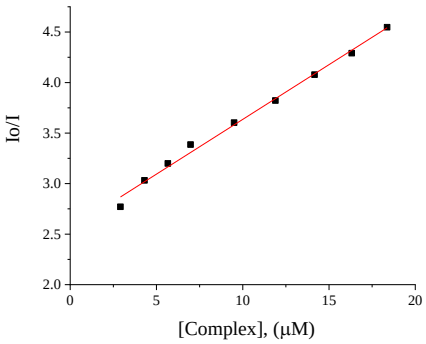

Complex **5**

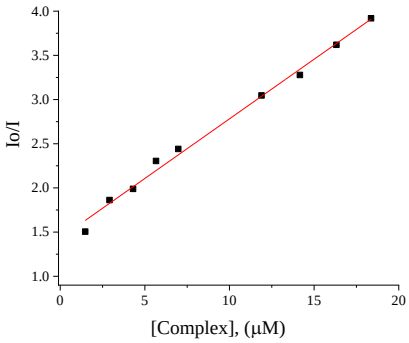

Complex **6**

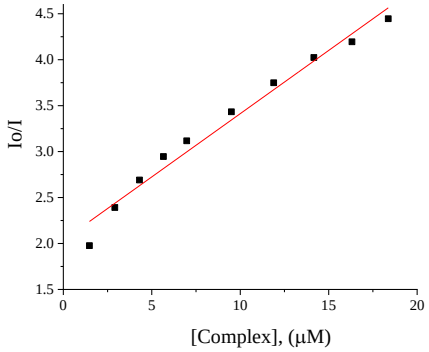

Complex **7**

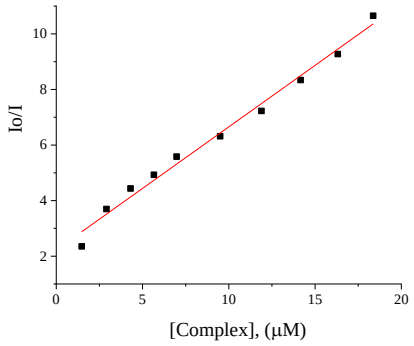

Complex **8**

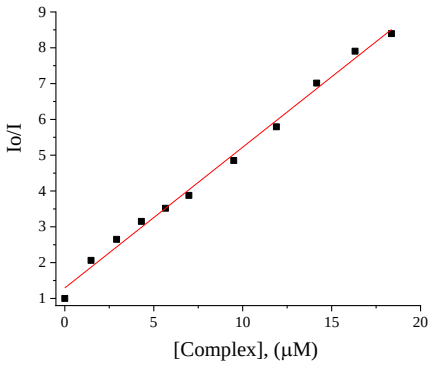

Complex **9**

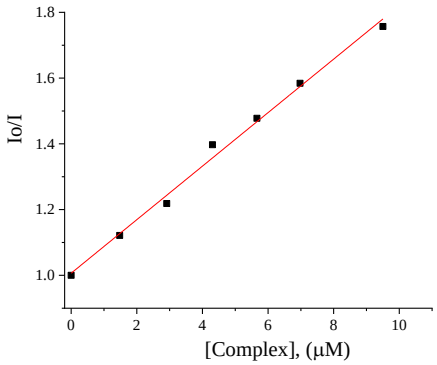

Complex **10**

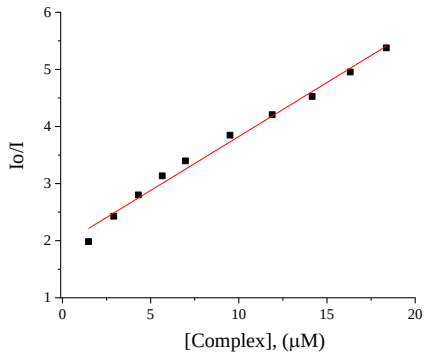

Complex **11**

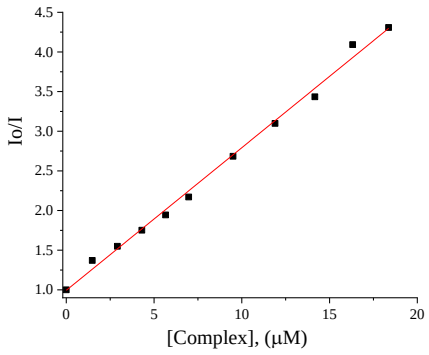

Complex **12**

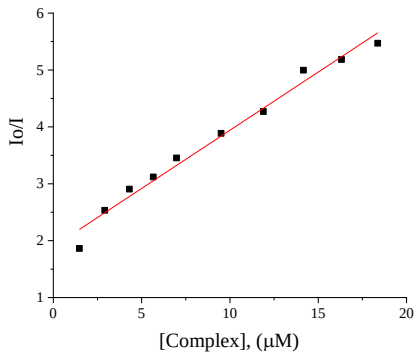

Complex **13**

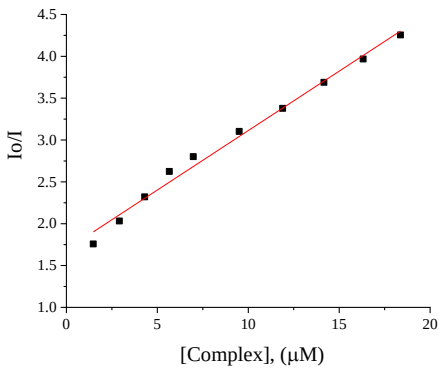

Complex **14**

Figure S10. Stern-Volmer plots of the HSA quenching experiments upon addition of complexes **1-14**.

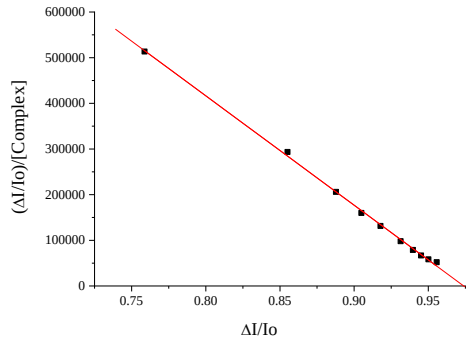

Complex **1**

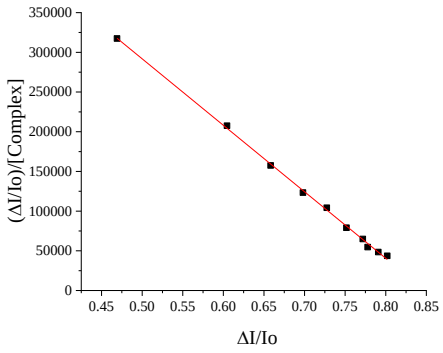

Complex **2**

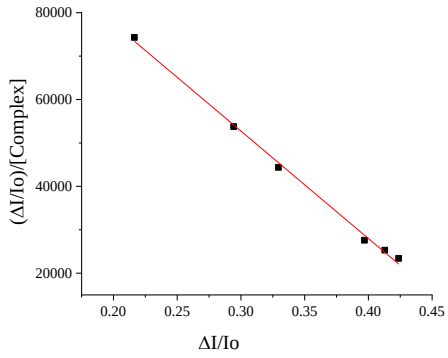

Complex **3**

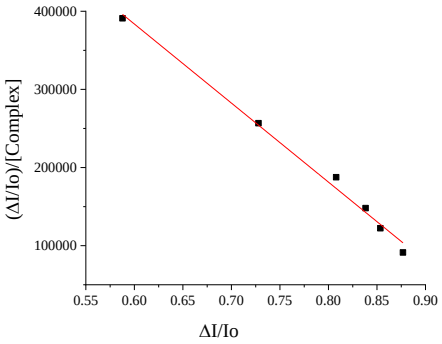

Complex **4**

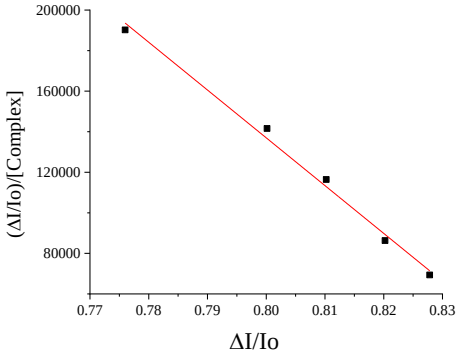

Complex **5**

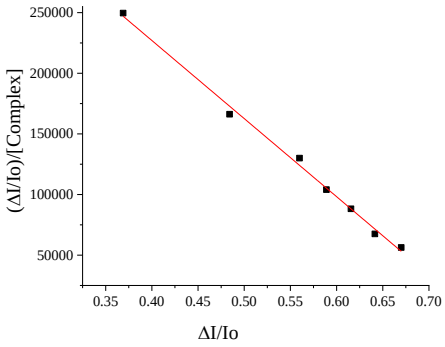

Complex **6**

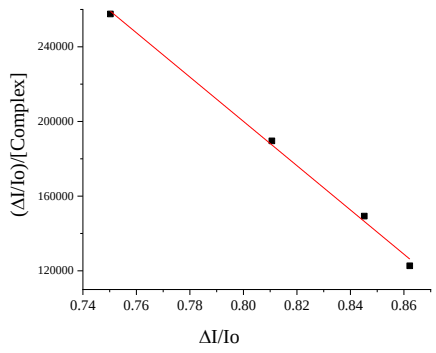

Complex **7**

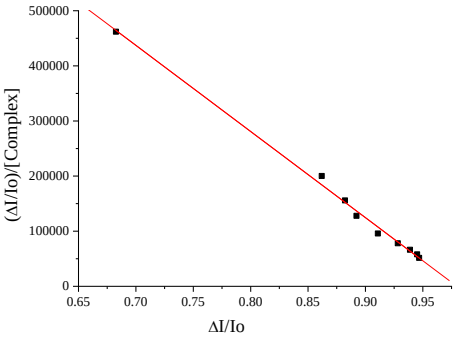

Complex **8**

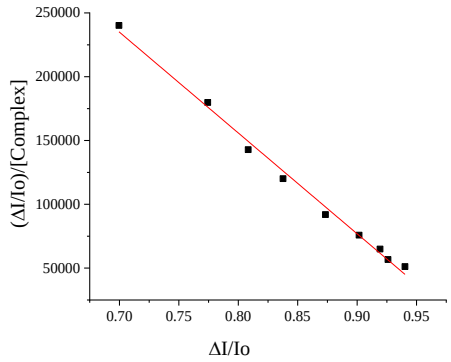

Complex **9**

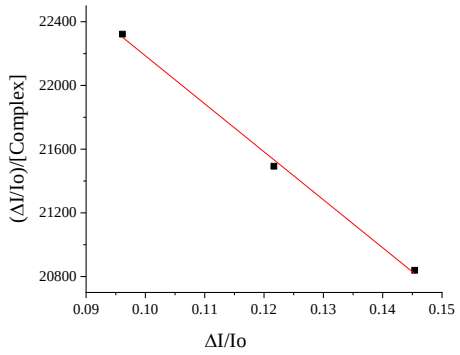

Complex **10**

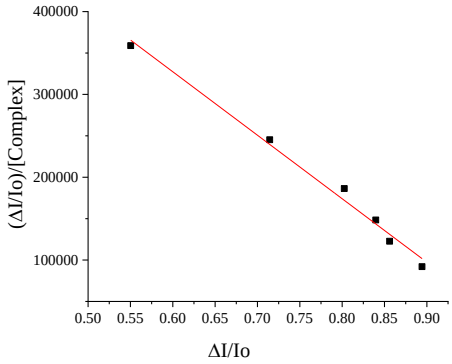

Complex **11**

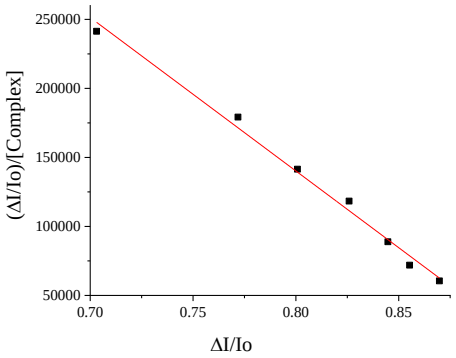

Complex **12**

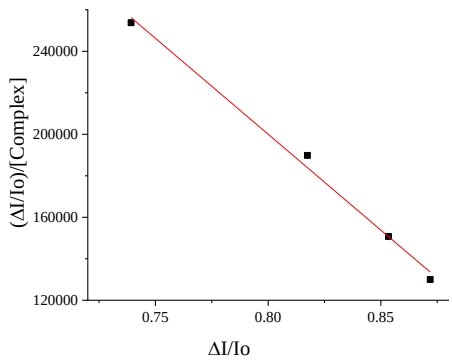

Complex **13**

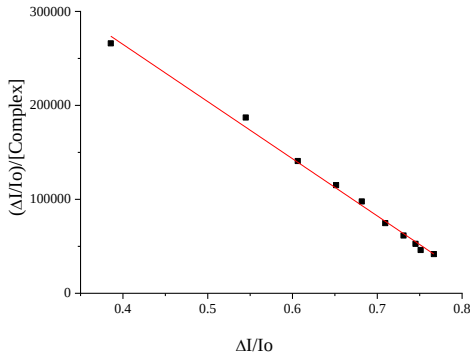

Complex **14**

Figure S11. Scatchard plots of the BSA quenching experiments upon addition of complexes **1-14**.

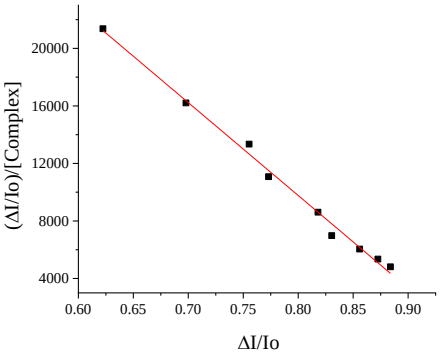

Complex **1**

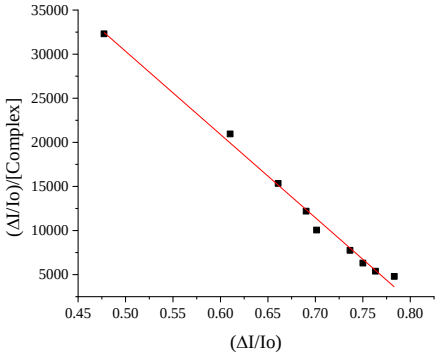

Complex **2**

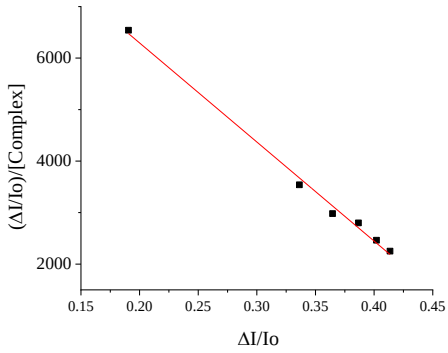

Complex **3**

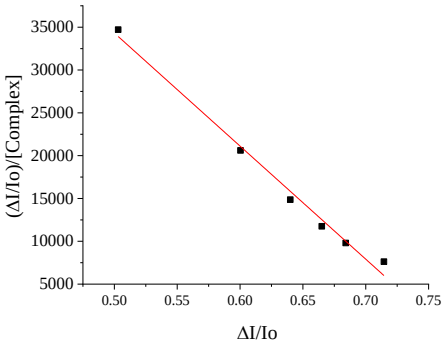

Complex **4**

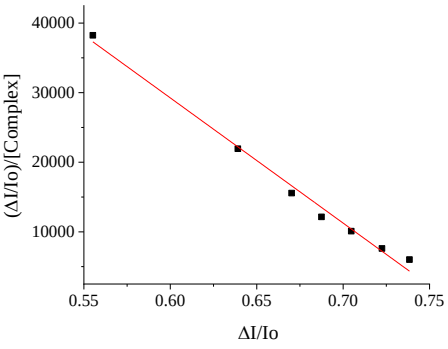

Complex **5**

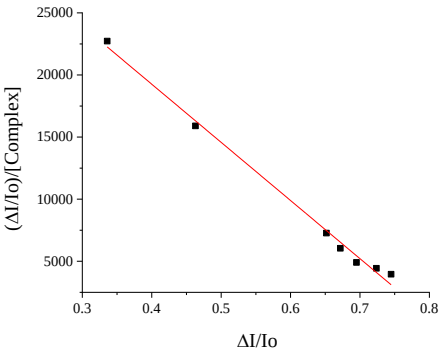

Complex **6**

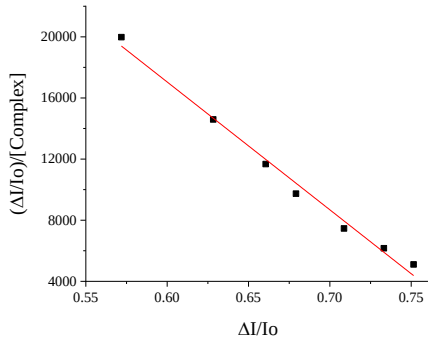

Complex **7**

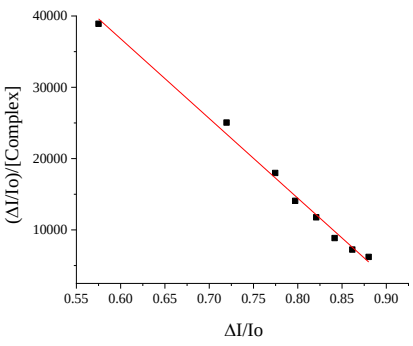

Complex **8**

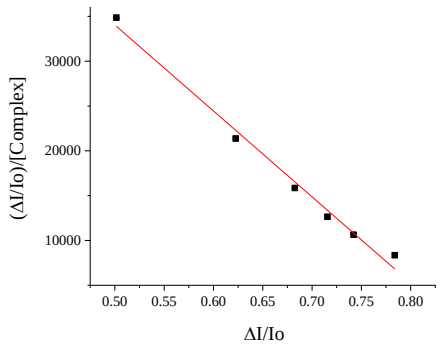

Complex **9**

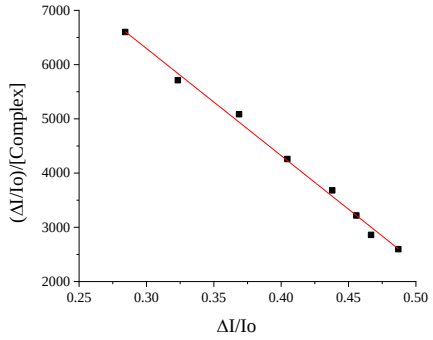

Complex **10**

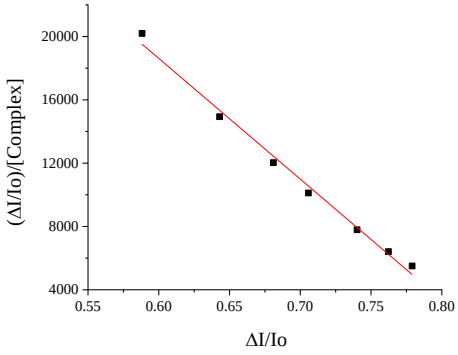

Complex **11**

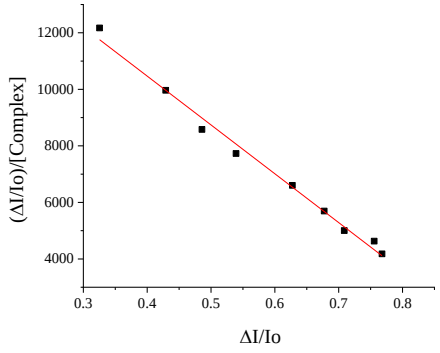

Complex **12**

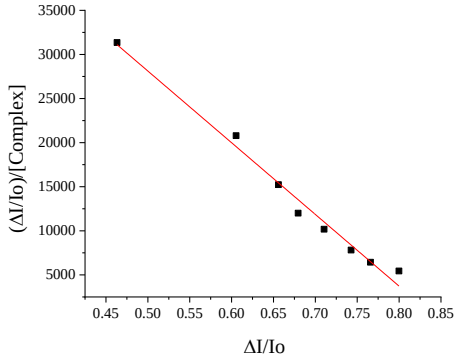

Complex **13**

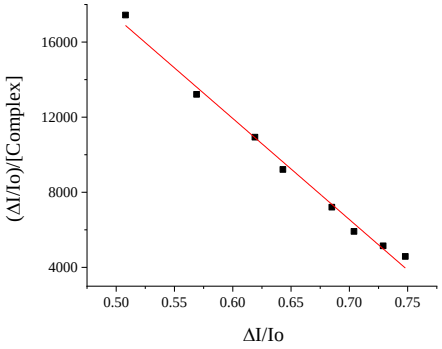

Complex **14**

Figure S12. Scatchard plots of the HSA quenching experiments upon addition of complexes **1-14**.

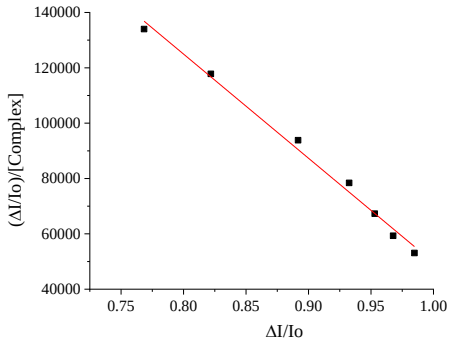

Complex **1**

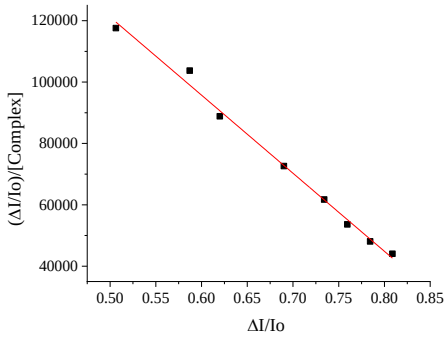

Complex **2**

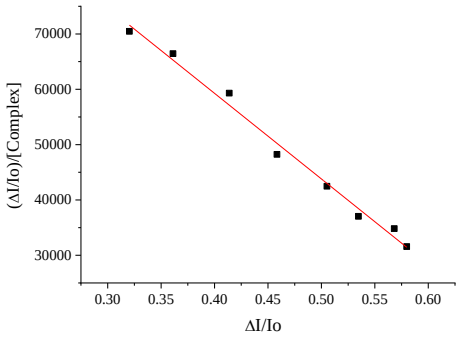

Complex **3**

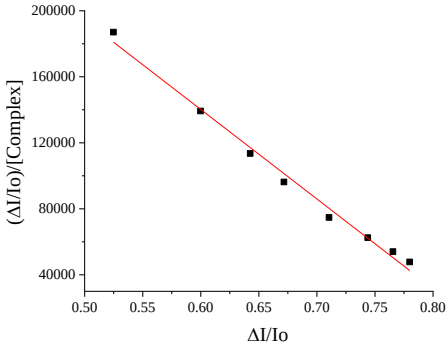

Complex **4**

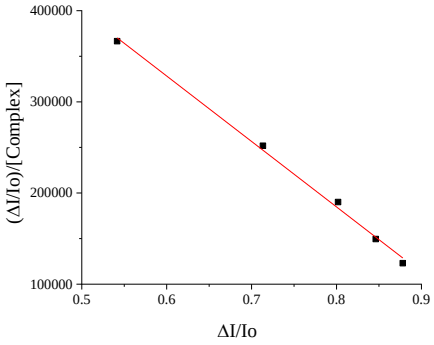

Complex **5**

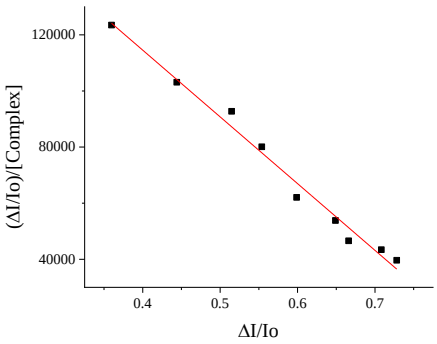

Complex **6**

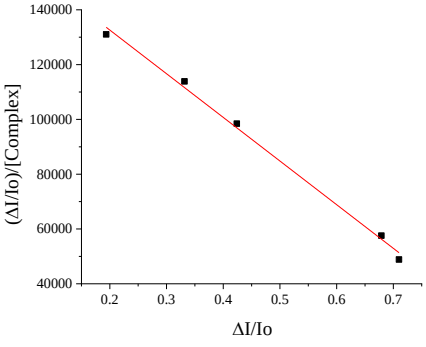

Complex **7**

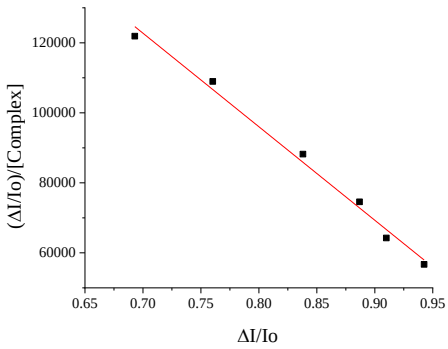

Complex **8**

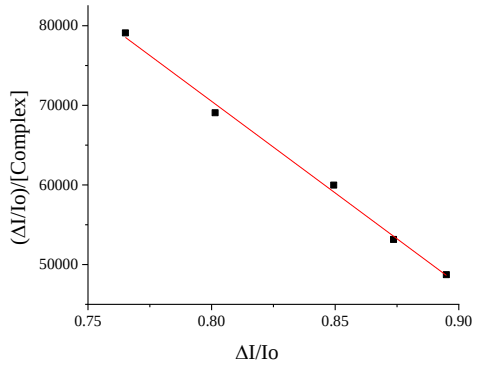

Complex **9**

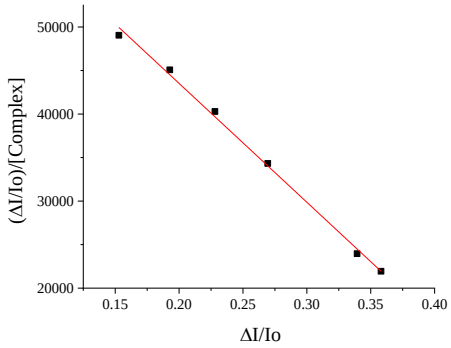

Complex **10**

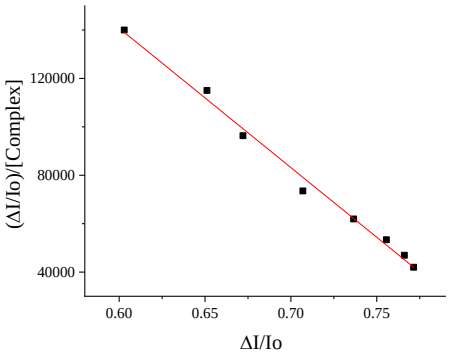

Complex **11**

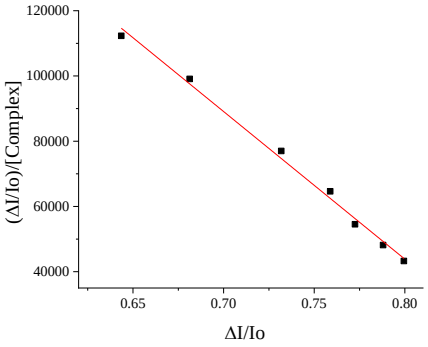

Complex **12**

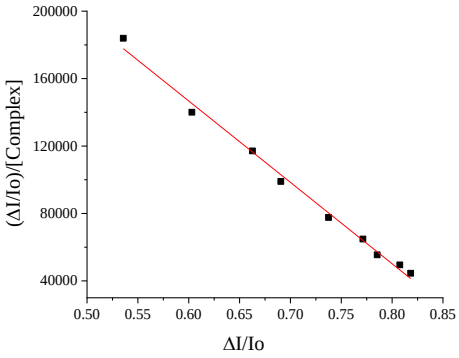

Complex **13**

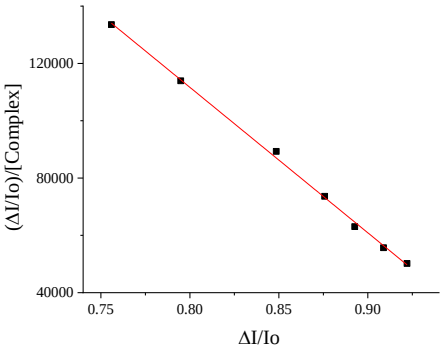

Complex **14**

Figure S13. Scatchard plots of the BSA quenching experiments in the presence of warfarin upon addition of complexes **1-14**.

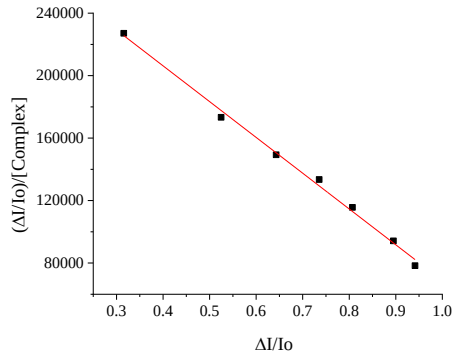

Complex **1**

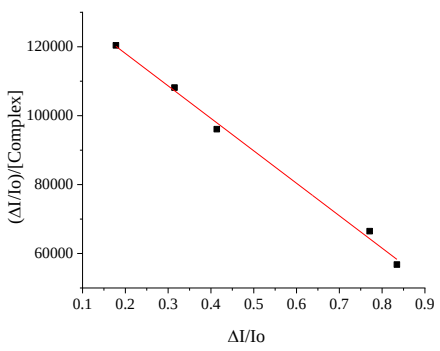

Complex **2**

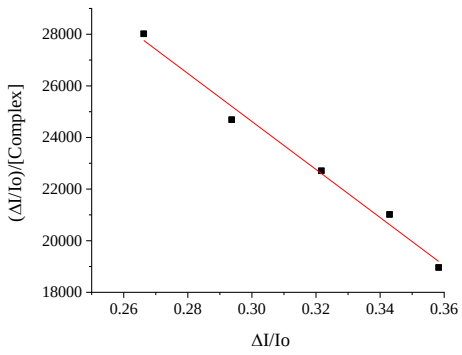

Complex **3**

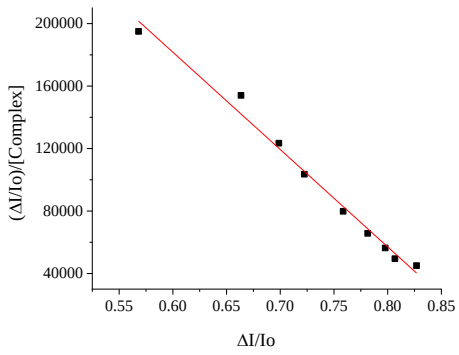

Complex **4**

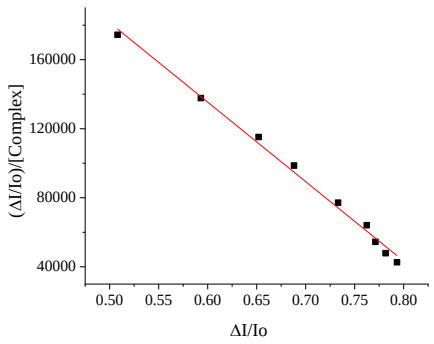

Complex **5**

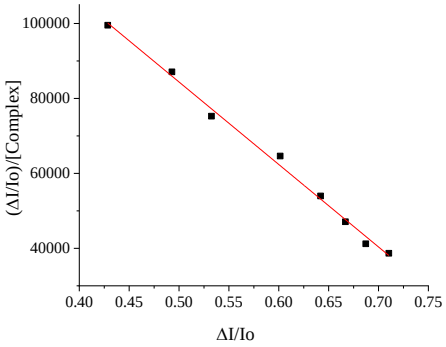

Complex **6**

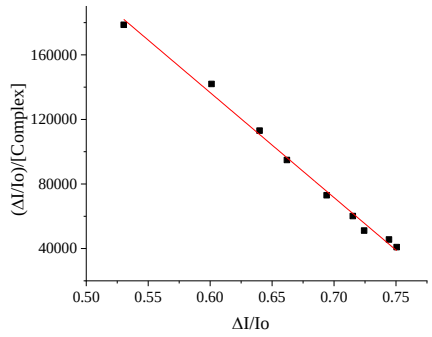

Complex **7**

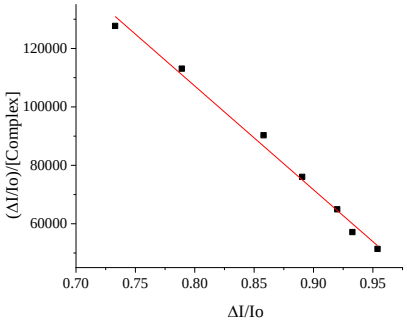

Complex **8**

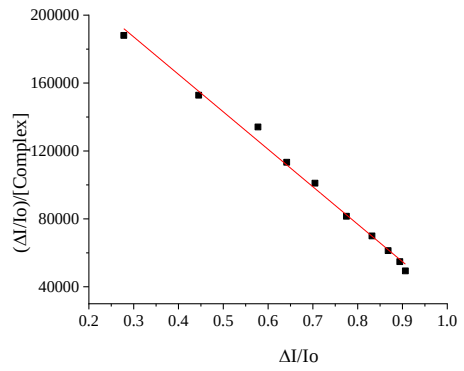

Complex **9**

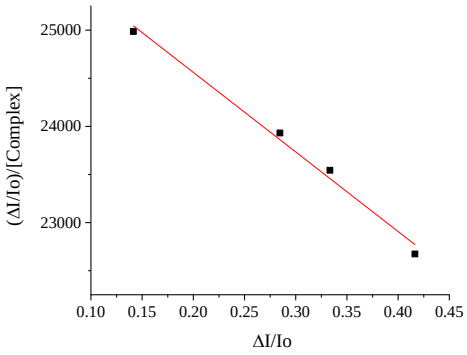

Complex **10**

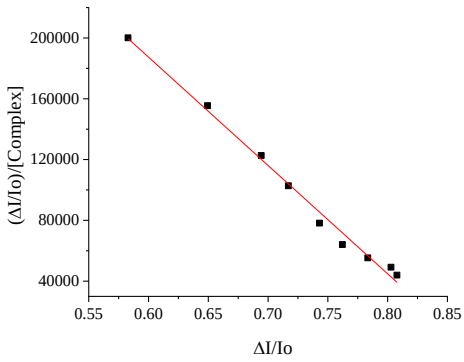

Complex **11**

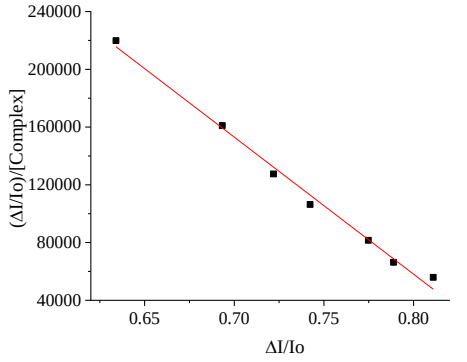

Complex **12**

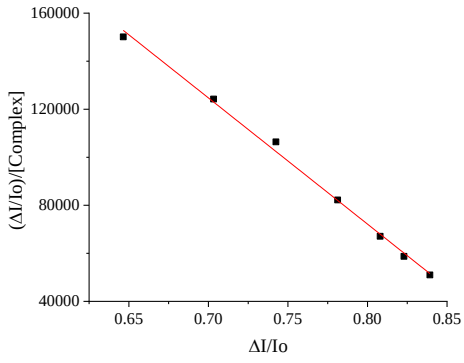

Complex **13**

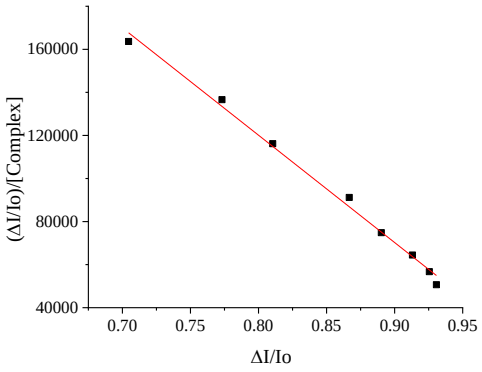

Complex **14**

Figure S14. Scatchard plots of the BSA quenching experiments in the presence of ibuprofen upon addition of complexes **1-14**.